Neurobiology of Disease 132 (2019) 104590

Contents lists available at ScienceDirect

Neurobiology of Disease

journal homepage: www.elsevier.com/locate/ynbdi

TrkB agonistic antibodies superior to BDNF: Utility in treating motoneuron degeneration

Wei Guo[a,b,1], Keliang Pang[a,b,1], Yanbo Chen[a], Shudan Wang[a,b], Heng Li[d], Yihua Xu[a,b], Fang Han[a,b], Hongyang Yao[a], Hang Liu[a,b], Vanessa Lopes-Rodrigues[e,f], Dang Sun[a], Jingyu Shao[a], Jianying Shen[a,g], Yang Dou[a], Wen Zhang[a], He You[a], Wutian Wu[c,d], Bai Lu[a,b,*]

[a] School of Pharmaceutical Sciences, IDG/McGovern Institute for Brain Research, Tsinghua University, Beijing 100084, China
[b] R&D Center for the Diagnosis and Treatment of Major Brain Diseases, Research Institute of Tsinghua University in Shenzhen, Shenzhen, Guangdong 518057, China
[c] Guangdong-Hong Kong-Macau Institute of CNS Regeneration, Jinan University, Guangzhou, Guangdong Province, China
[d] School of Biomedical Sciences, Division of Anatomy, The University of Hong Kong, Pokfulam, Hong Kong Special Administrative Region, China
[e] Department of Physiology, National University of Singapore, Singapore
[f] Life Sciences Institute, National University of Singapore, Singapore
[g] Artemisinin Research Center, Institute of Chinese Materia Medica, China Academy of Chinese Medical Sciences, Beijing 100084, China

ARTICLE INFO

Keywords:
Receptor tyrosine kinase
Neurotrophin
BDNF
TrkB signaling
Agonistic antibody
Monoclonal antibody
$p75^{NTR}$
Drug discovery
Motoneuron degeneration
ALS

ABSTRACT

While Brain-derived Neurotrophic Factor (BDNF) has long been implicated in treating neurological diseases, recombinant BDNF protein has failed in multiple clinical trials. In addition to its unstable and adhesive nature, BDNF can activate $p75^{NTR}$, a receptor mediating cellular functions opposite to those of TrkB. We have now identified TrkB agonistic antibodies (TrkB-agoAbs) with several properties superior to BDNF: They exhibit blood half-life of days instead of hours, diffuse centimeters in neural tissues instead millimeters, and bind and activate TrkB, but not $p75^{NTR}$. In addition, TrkB-agoAbs elicit much longer TrkB activation, reduced TrkB internalization and less intracellular degradation, compared with BDNF. More importantly, some of these TrkB-agoAbs bind TrkB epitopes distinct from that by BDNF, and work cooperatively with endogenous BDNF. Unlike BDNF, the TrkB-agoAbs exhibit a half-life of days/weeks and diffused readily in nerve tissues. We tested one of TrkB-agoAbs further and showed that it enhanced motoneuron survival in the spinal-root avulsion model for motoneuron degeneration *in vivo*. Thus, TrkB-agoAbs are promising drug candidates for the treatment of neural injury.

1. Introduction

Neurotrophins are highly homologous, dimeric neurotrophic factors comprised of nerve growth factor (NGF), brain-derived neurotrophic factor (BDNF), neurotrophin-3 (NT-3), neurotrophin-4/5 (NT-4/5) (Chao, 2003; Kaplan and Miller, 2000; Lewin and Barde, 1996). These are secretory proteins that are initially synthesized as precursors (pro-neurotrophins), which are cleaved by either intracellular or extracellular proteases to produce mature neurotrophins. The mature neurotrophins bind and activate the Trk (tropomyosin receptor kinase) family of receptor tyrosine kinases (Friedman and Greene, 1999; Ibanez, 1998; Nagappan and Lu, 2005). Among all neurotrophins, BDNF and its receptor TrkB have received the most attention for their high expression levels and diversified functions in the central nervous system (CNS). It is believed that mature BDNF exists as stable dimers to draw two TrkB receptor monomers together. The receptor dimerization results in auto-phosphorylation on the tyrosine residues of TrkB intracellular domain, leading to the activation of multiple signaling cascades, including the Ras/extracellular regulated kinase (Erk) pathway, phosphatidylinositol-3 kinase (PI3 kinase)/Akt pathway and PLCγ/PKC pathway (Huang and Reichardt, 2001; Kaplan and Miller, 2000). These signaling events ultimately bring about a series of cellular functions, such as enhancing neuronal survival and differentiation during brain development, maintaining synaptic connections and modulating synaptic transmission and plasticity in the adult brain (Greenberg et al., 2009; Huang and Reichardt, 2003; Lewin and Barde, 1996; Reichardt, 2006). ProBDNF and sometimes high concentrations of mBDNF can also bind and activate p75 neurotrophin receptor ($p75^{NTR}$) (Chao, 1994, 2003; Hempstead, 2002). The signaling cascades downstream of TrkB and $p75^{NTR}$ often lead to opposing biological functions in the nervous

* Corresponding author at: School of Pharmaceutical Sciences, Room B303, Tsinghua University, Beijing 100084, China.
E-mail address: bai_lu@tsinghua.edu.cn (B. Lu).
[1] These authors have contributed equally to this work.

https://doi.org/10.1016/j.nbd.2019.104590
Received 7 July 2019; Received in revised form 18 August 2019; Accepted 26 August 2019
Available online 27 August 2019
0969-9961/

system. While activation of TrkB is crucial for neuronal survival and synaptic potentiation, $p75^{NTR}$ signaling is often associated with cell death and synaptic depression (Frade et al., 1996; Woo et al., 2005). A Yin/Yang theory of neurotrophins was therefore proposed (Lu et al., 2005). It is critical to determine whether the TrkB or $p75^{NTR}$ signaling is activated when studying the physiological functions of BDNF *in vivo*.

The BDNF-TrkB signaling pathway has recently been postulated as a drug target for the treatment of neurological diseases, including nerve injury and neurodegenerative diseases, and neuropsychiatric disorders such as major depression (Autry and Monteggia, 2012; Lu et al., 2013; Nagahara and Tuszynski, 2011). Spinal motoneuron degeneration is the critical pathophysiology involved in Amyotrophic lateral sclerosis (ALS), a devastating neurodegenerative disease and has no disease-modifying therapy. (Gordon, 2013; Mitchell and Borasio, 2007). The acute model for motoneuron degeneration caused by spinal root injuries could be rescued by enhancing BDNF-TrkB signaling (Giehl and Tetzlaff, 1996; Kishino et al., 1997; Sendtner et al., 1992; Tuszynski et al., 1996; Yan et al., 1992). Spinal root avulsion and axotomy were both used for modeling the acute motoneuron degeneration. Two early reports showed that BDNF rescued spinal motoneuron from axotomy-induced cell death (Sendtner et al., 1992; Yan et al., 1992). However, axonal injury, especially the distal axotomy, usually did not induce significant motoneuron death. It has been shown that 4 mm of remaining peripheral nerve is sufficient for preserving motoneuron survival (Gu et al., 1997). Therefore, spinal root avulsion model was considered as a more promising acute model for motoneuron degeneration (Ruven et al., 2014). In this model, spinal root was completely removed from motoneuron, causing nerve injury of both peripheral (Wallerian degeneration) and central (spinal motoneuron) system. Motoneuron degeneration has been ascribed to the failure of retrograde axonal transport of neurotropic substances including BDNF. Meanwhile, BDNF has been shown to prevent cell death of motoneuron in spinal root avulsion model (Kishino et al., 1997; Wu et al., 2003). However, in rodent SOD1 transgenic models of ALS, administration of BDNF did not attenuate the disease progression (Lowry et al., 2001). More importantly, intra-muscle (Neurology, 1999) or intrathecal delivery of recombinant BDNF protein failed to generate positive outcomes in ALS clinical trials (Ochs et al., 2000). Failures in the clinical utility of BDNF in ALS were attributed to several reasons (Henriques et al., 2010). First, the blood half-life of BDNF protein is extremely short, only 1–10 min in the plasma (Poduslo and Curran, 1996; Sakane and Pardridge, 1997) and 1 h in CSF (Soderquist et al., 2009). Second, the physicochemical properties of BDNF have made the recombinant protein difficult to diffuse (isoelectric point, pI ≈10). BDNF protein delivered intraventricularly or through midbrain infusion remained in the injection site without penetrating into the brain tissue (Croll et al., 1998; Morse et al., 1993). Third, the high local concentration of BDNF may activate $p75^{NTR}$ which is prominently expressed in dying motoneurons, raising further concerns about the benefits of BDNF delivery (Dittrich et al., 1996; Knusel et al., 1997).

To overcome the intrinsic problems of BDNF, one may attempt to develop new TrkB agonists. Several small-molecule compounds were reported to induce TrkB activation and could be potentially used as therapeutics of neurodegenerative diseases (Jang et al., 2010; Longo and Massa, 2013). However, two recent studies have systematically examined these molecules and concluded that they neither bind nor activate TrkB receptor, raising serious doubts on the utilities of these molecules (Boltaev et al., 2017; Todd et al., 2014). Additionally, from a structural point of view, it may be extremely challenging, if not unfeasible, for small molecules to induce TrkB activation: chemical compounds are generally too small to be able to bridge the two TrkB monomers. An alternative approach is to generate TrkB agonistic antibodies, which, similar to BDNF dimer, may bring the two TrkB monomers together to induce its activation. Several agonistic antibodies have been developed. These antibodies can bind TrkB and activate its tyrosine kinase *in vitro* (Merkouris et al., 2018; Qian et al., 2006; Todd et al., 2014; Traub et al., 2017). In one study, a TrkB antibody has been shown to induce activation of TrkB downstream signaling and exert neuroprotection in the developing brain after hypoxic ischemia in perinatal animals (Kim et al., 2014). Intra-ocular injection of another TrkB antibody delayed retinal ganglion cell death in animal models of complete optic nerve axotomy or ocular hypertension (Bai et al., 2010). However, it is unclear where on the TrkB extracellular domain they bind, whether they possess unique features compared to BDNF, or how they behave in the brain *in vivo*.

In the present study, we aim to develop TrkB agonistic antibodies with drug-like properties. We used the highly sensitive NFAT assay (Boltaev et al., 2017; Merkouris et al., 2018; Todd et al., 2014) and established a TrkB-Tyr515 phosphorylation AlphaLISA assay to screen for agonistic antibodies and to evaluate their pharmacological properties. We looked for agonistic antibodies that were not only specific and potent, but also highly stable in the blood and were non-competitive to endogenous BDNF. We discovered that among about 30 agonistic antibodies, some activated TrkB with prolonged kinetics and superior pharmacokinetic properties, and they worked non-competitively or even cooperatively with BDNF. We have examined the efficacy of one representative antibody, Ab4B19, on neuronal death in both *in vitro* and *in vivo* models (Graham, 2002; Kishino et al., 1997). Our results suggest that TrkB-agoAbs have the potential to be developed into therapeutics for the treatment of neurological disorders including neurodegenerative diseases.

2. Materials and methods

2.1. Protein expression and purification

The TrkB-ECD430 gene fragment (corresponding to the amino acids from 30 to 430, namely the full-length extracellular domain) of the human or rat TrkB (hTrkB or rTrkB) gene was cloned into pFastBac Dual with human Fc or 6 × His tags on the C terminal. Baculovirus containing the above TrkB-ECD genes was produced using the Bac-to-Bac system from Invitrogen. After infecting the SF9 cells, the culture was incubated at 27 °C in the MSF1 media. After 72 h of incubation, supernatant of the culture was collected and centrifuged under 4 °C at 4000 rpm for 20 min. After the collection of supernatant, Nickel column (70501–5, Beaver) and gel filtration chromatography (uperdex200, 17,517,501, GE) were used for protein purification. The nickel column was balanced with 1 × TBS buffer before loading the supernatant containing target proteins. While the target protein binds the column specifically, non-specific proteins were washed away by 1 × TBS buffer. The target protein was eluted with concentrated imidazole buffer. The eluent was then loaded onto the molecular sieve where high-molecular-weight proteins were eluted earlier than the low-molecular-weight proteins.

2.2. Production of mouse monoclonal antibodies by the hybridoma technology

1) Antigen Preparation

The coding sequence of TrkB extracellular domain was cloned into the Pfastbac vector containing a signal peptide, and the protein was purified from the insect sf9 cell line. Three kinds of proteins with different tags were prepared: hTrkB-ECD-hFc for animal immunization, and hTrkB-ECD-His and rTrkB-ECD-His for screening.

2) Animal Immunization

The antigen (recombinant TrkB-ECD-hFc) was dissolved in DPBS and used to immunize BALB/C mice of about 6–8 weeks old *via* subcutaneous route injections. During the fast immunization procedure, these animals were immunized for about 8 times. All experiments

involving animals in this study were approved by Tsinghua University Committees on Animal Care.

3) Lymphocyte isolation

After immunization, animals were selected by tittering using ELISA. Briefly, the serum from immunized mice or naïve mice were added into the ELISA plate coated with TrkB-ECD-his protein. The titer of each mice was determined by the optical density at 450 nm (OD450) using ELISA. Immunized mice with the highest titer were sacrificed and lymph nodes were harvested. The lymphoid cells were suspended in DMEM before fusion with a myeloma cell line Sp2/0-Ag14.

4) Cell fusion

Lymphoid cells were fused with Sp2/0-Ag14 by PEG (P7306, sigma). The fused cells were suspended in HAT selecting medium (21060–017, Gibco). On day 7 or 10, one-half medium was changed.

5) Hybridoma high throughput screening and sub-cloning

After 14 days of culturing, hybridoma supernatants were screened for TrkB-specific monoclonal antibodies. ELISA was used to analyze the affinity of the antibodies, and NFAT assay was used to select active TrkB agonists. After selection of positive cell pools, sub-cloning was done by limiting dilution.

6) Monoclonal antibody isotype identification and hybridoma sequencing

ELISA Kit (BAT0296, Sino Biol.) was used to identify the isotype of the monoclonal antibodies. Hybridoma sequencing was performed with the 5'RACE kit (cat.634858, &634,859, Clontech).

2.3. Production of rabbit monoclonal antibodies by yeast display

Recombinant human TrkB-ECD was dissolved in DPBS and used to immunize rabbits of 6–8 weeks old *via* subcutaneous injections. After immunization, animals were selected for B cell preparation by titer ELISA. Immunized rabbits were sacrificed and lymph nodes were harvested. The B cell immunoglobulin repertoire of the immunized rabbit was immortalized by the combinatorial cloning of the rearranged variable domains of light (V-L) and heavy (V-H) chains, which were introduced into the yeasts and displayed on the yeast surface as the single chain FV (scFV). Affinity selection of the scFV antibodies with FACS was followed by reconstructing them into the complete template of the IgG. Further screening for agonist antibodies was carried out by NFAT assay.

2.4. ELISA

The recombined protein (40 μg/ml at 100 μl, the extracellular domain of TrkA, TrkB, TrkC or p75NTR) was used to coat the 96- well ELISA plate (Corning, cat.9018) overnight. After three washes using PBS, the TrkB agonistic antibody Ab4B19 (10 nM, 1 nM or 0.1 nM at 100 μl) was added into the wells, incubated for 2 h, and then washed 3 times with washing buffer. The HRP-labeled secondary antibody was added into the well and incubated for 30 min. After another 3 washes, 100 μl of chromogenic substrate was added into the wells. The plate was kept in the dark at room temperature for 30 min and 100 μl of stop solution was added into each well to stop reaction. The absorbance of each well was read at 450 nm by microplate reader (Biotek, Cytation5) and indicated the binding activity.

2.5. NFAT

Experiments were carried out following the protocol provided by LiveBLAzer™ FRET-B/G Loading Kit (K1095, Life Technologies). The day before experiment, *Cellsensor* TrkB-NFAT-bla CHO-K1cells (K1435, Life Technologies) were seeded in 384-well plates with 32 μl media. After 5 h of BDNF or TrkB-agoAb treatment at 37 °C, the culture was incubated for 2 h at room temperature with 8 μl substrate. Cell-free wells were used as the background. FRET signals (405 nm excitation, 460 nm & 530 nm emission) were obtained from the microplate reader (Envision, PerkinElmer) and background signals were subtracted. The ratio of fluorescent signals at 460 nm to 530 nm reflected the level of TrkB activation. The level of TrkB activation by each treatment was normalized to that by vehicle treatment. More details could be found in the handbook for LiveBLAzer™ FRET-B/G Loading Kit (K1095, Life Technologies). Data was qualified using GraphPad Prism.

2.6. Cell line culture

All the cells were incubated in 37 °C 5% CO_2 cell incubator. CHO cells were cultured in FK-12K medium (21127–022, Gibco) supplemented with 10% FBS (16,000,044, Life technology). PC12 cells were cultured in DMEM medium supplemented with 5% FBS, 10% horse serum (HS). The complete medium of primary neurons and medium for SH-SY5Y cells was DMEM medium supplemented with 10% FBS and 1% GlutaMAX-I (35,050,061, Gibco). Maintenance medium of primary neurons was Neurobasal (10,888,022, Gibco) medium supplemented with 2% B-27 and 1% GluMAX-I. All these mediums were supplemented with 0.2% penicillin and streptomycin. hTrkB-CHO cells were cultured in the medium containing 5 μg/ml blasticidin (R210–01, invitrogen). To passage the cells, HBSS was used to wash off the medium, and 0.05% EDTA trypsin was used to digest cells.

2.7. AlphaLISA

AlphaLISA for detecting TrkB Y515 phosphorylation was established based on a sensitive homogeneous AlphaLISA/AlphaScreen assay from PerkinElmer (6,760,617M). The day before experiment, *Cellsensor* TrkB-NFAT-bla CHO-K1cells (K1435, Life Technologies) were seeded in 96-well plates with 200 μl media. After treatment of BDNF or TrkB-agoAb, the cells were washed by cold PBS for 3 times and were lysed in the buffer containing 50 mM Tris–HCl (pH 8.0), 250 mM NaCl, 1% NP-40, 0.5% deoxycholate, 0.1% SDS, and protease inhibitors (Roche Diagnostics) for 30 min on ice. In white opaque plates, 10 μl donor bead (6,760,617 M, PerkinElmer) and 10 μl biotinylated anti-TrkB monoclonal antibody (BAF397, R&D) were added in each well and incubated for 30 min at 37 °C under subdued light. Then, 10 μl lysate, 10 μl anti-pTrkB antibody (ab51187, Abcam) and 10 μl acceptor beads (6,760,617 M, PerkinElmer) were added into the according wells and incubated for 1 h at 37 °C under subdued light. Lysate-free wells with all reagents were used as the background. Signals were measured with Envision (PerkinElmer) and background signals were subtracted. The relative levels of TrkB activation were determined by the ratio of the signals by each treatment to that by vehicle treatment. Data were analyzed and plotted using GraphPad Prism afterwards.

2.8. Biacore (SPR) (Biacore T200, GE)

CM5 chip was washed in PBS with sonication. The buffer of candidate antibodies and the target protein was replaced with the same PBS. The target protein was diluted to 1 μg/μl as the solid phase and the candidate antibodies were serial diluted to 7 dilutions as the fluid phase. After obtaining the signal, Biacore Evaluation Software was used to create fitting curves for the responses (Resonance Units, RU). ch2 < Rmax/10 indicated good confidence level.

2.9. Truncated TrkB construction, transfection and Co-IP

The truncated TrkB (shown in Fig. 2C) gene was cloned into pcDNA3.1 with GFP tag on the C-terminal. The endotoxin-free plasmids were transfected into normal CHO cells using Lipofectamine2000 kit (11668–019, Invitrogen). The empty vector of pcDNA3.1 was used as the control. All the operations followed the instruction manual. Opti-MEM (31985–070, Invitrogen) was used to dilute plasmid and lipofectamine 2000 (11668–019, Invitrogen), respectively. The diluted plasmid was mixed with Lipofectamine2000 gently and incubated for 30 min at room temperature. The mixture was then applied to the cells. After 24-hour incubation, the transfected cells were lysed by RIPA solution as shown above. Different TrkB-agoAbs were added into lysates overnight at 4 °C, followed by 20 ul protein A/G beads incubation for 4 h. After three times of washing by RIPA solution with intervals of 10 min, 20 ul loading buffer was added into tubes and denatured at 95 °C for 5 min. Western blotting was performed to analyze the binding properties.

2.10. SDS-PAGE and Western blotting

Cells were washed by cold PBS for 3 times and were lysed in buffer containing 50 mM Tris–HCl (pH 8.0), 250 mM NaCl, 1% NP-40, 0.5% deoxycholate, 0.1% SDS, and protease inhibitors (Roche Diagnostics) for 30 min on ice. After centrifugation to remove insoluble material, the proteins in lysate were separated using10% SDS–PAGE, and transferred to a PVDF membrane (Immobilon-P, Millipore). The membrane was blocked with 5% BSA in Tris buffered saline with 0.1% Tween (TBST) and incubated overnight at 4 °C with the antibody diluted in 5% BSA in TBST. Membranes were washed with TBST, incubated with secondary antibodies, washed with TBST, and detected with SuperSignal West Pico Chemiluminescent substrate (34,080, Pierce). The primary antibodies used in Western blotting were described previously (Guo et al., 2014).

2.11. Survival assay using hTrkB-PC12 cells

PC12 cells expressing human TrkB were cultured in 96-well plates (20000cells/well) overnight in 1640 medium with 10% horse serum and 5% fetal bovine serum. To preserve hTrkB expression, 200 μg/ml G418 was supplemented. Then the medium was changed to serum-free 1640 medium in the present or absent of TrkB agonist or TrkB agonist plus the inhibitor k252a or AZD-1332 at 100 μl/well. The wells with serum supplemented medium were considered as the positive control. NucViewTM 488 Caspase-3 substrate (Biotium, 30,029) was prepared by a 10-fold dilution. After 16 h of treatment, 10 μl diluted substrate was added into each well and incubated for 15 min at room temperature. Fluorescence at 488 nm (Caspase-3) positive cells and total cells were counted with high content technology (Cellomics, Thermo). Apoptotic level (AL) of each group was determined by the ratio of the number of Caspase-3 positive cells to total number of cells. Survival rates by the treatment of TrkB agonists with or without the Trk inhibitor were calculated as below:

$$\text{Survival rate} = \frac{AL\,(treatment) - AL(serum\ free)}{AL\,(serum\ supplemented) - AL(serum\ free)}$$

2.12. Homo-FRET anisotropy microscopy

Anisotropy microscopy was done as previously described (Lin et al., 2015) in COS-7 cells that were transiently transfected with a rat $p75^{NTR}$-EGFP* fusion construct as previously described (Vilar et al., 2009). EGFP* denotes a monomeric A207K EGFP mutant. Changes in anisotropy were expressed as fold change at each time point in comparison to the mean of 6 time points obtained prior to addition of vehicle, TrkB-agoAb4B19 (3 nM) or BDNF (3 nM).

2.13. TrkB agonist diffusion in spinal cord

C57BL/6 mice (8–10 weeks) were anesthetized with avertin (i.p.). A scission on the skin around the spinal cord was made to expose the injection point. A micro-syringe was slowly inserted into the L2-L3 lumbar spine until the mouse tail flicked. FITC-labeled TrkB agonists (5 μg in 5 μl) were then injected into the spinal cord slowly. 24 h later, the spinal cords were isolated and the frozen sections were imaged using a confocal microscope.

2.14. Motoneuron culture and cell death assay

E13 pregnant mice were euthanatized by cervical dislocation. The embryos were carefully removed from the uterus and kept in ice-cold HBSS. After decapitation, the embryo was placed with the dorsal side up. The outer thin sheath of skin was removed and the central channel of the spinal cord was opened with a pair of tweezers. The isolated spinal cord was transferred to a new Neurobasal medium-containing dish and was placed with the dorsal upwards. The dorsal root ganglia (DRG) and the ensheathing meninges were remove. The isolated spinal cords were chopped into small pieces, and was incubated for 20 min at 37 °C in digestion solution (papain and DNase in Neurobasal medium). The digestion solution was discarded after centrifugation, and the cell aggregates were gently triturate with a 5 ml pipette in fresh Neurobasal medium. The resulting suspension was first centrifuged for 5 min at 600 rpm at RT to remove cell debris. Then motoneurons were enriched using Optiprep (D1556, Sigma, USA)-based density gradient centrifugation modified from published protocol by Graham (Graham, 2002). The supernatant was discarded, the pellet was re-suspended in HBSS, and the suspension was layered over a cushion of 3 ml 10.4% (*w/v*) Optiprep and centrifuged for 400 ×*g* 25 min at room temperature. The top layer enriched in motoneurons was collected, then 10 ml Neurobasal medium was added and then centrifuged for 10 min at 1200 rpm at RT to collect cells. The cell pellet was finally suspended in motoneuron complete medium (10% horse serum, 1× B27, and 1× GlutaMax in Neurobasal). An appropriate number of cells were plated on PDL and laminin-coated dishes or coverslips. After cells attached to the surface of the culture dish, the medium was carefully replaced with complete medium (containing neurotrophic factors or antibodies).

Cell death was measured using *in situ* cell death detection kit (11,684,795,910, Roche) following instruction. Briefly, cells were fixed with 4% PFA in PBS for 20 min and permeabilized with 0.1% Triton for 10 min, then incubated in TUNEL reaction solution. ChAT and fluorescein double-labeled cells were counted using high content scanning and analysis system.

2.15. Immunocytochemistry

Cholinergic motoneurons can be identified by high expression level of choline acyltransferase (ChAT) (Camu & Henderson, 1992). Cells were fixed with 4% PFA in PBS for 20 min, and immunostaining was carried out following standard protocol with a goat anti-ChAT antibody (AB143, Merk millipore, USA). The purity of motoneuron culture was assessed by determining the percentage of labeled cells. Neurite number and length were determined after immunolabelling cells with an antibody against neuronal class III b-tubulin (AT-809, Beyotime Biotechnology, China). Neurite length was measured using high content scan and analysis system (ArrayScan VTI 700, Thermo, USA), following neuronal profile V4 protocol.

2.16. Spinal root avulsion injury

Adult female Sprague Dawley (SD) rats (250 to 300 g body weight, 70 to 90 days old) were used in this study. Animals were anesthetized

with a mixture of ketamine (80 mg per kg of body weight) and xylazine (8 mg per kg), by intraperitoneal injection. The right spine segments from the 5th to the 7th cervical (C5-C7) were exposed. A dorsal laminectomy was performed on lamina C6 to expose the C7 dorsal root. After opening the dura matter, the right side C7 roots (both dorsal and ventral) were avulsed using a fine glass hook. Another cut was made on the distal C7 spinal nerve and the disconnected C7 dorsal and ventral roots, together with a small fragment of spinal nerve, were removed. Immediately, a gelfoam soaked with 5 μg BDNF, 5 μg TrkB-agoAb4B19 or same volume of PBS was gently placed onto the injured spinal cord surface. After that, an osmotic minipump, filled with the same solution as in the gelfoam, was embedded subcutaneously near the injury site. The pump was connected with a tube, which led the released drugs to the injured spinal cord surface. Grouping and sample sizes are shown below:

1) Sham ($N = 7$): no avulsion + gelfoam (with 5 μl PBS) + pump (releasing 12 μl PBS per day)
2) PBS treated negative control (N = 7): C7 avulsion + gelfoam (with 5 μl PBS) + pump (releasing 12 μl PBS per day)
3) BDNF treated positive control ($N = 8$): C7 avulsion + gelfoam (with 5 μg BDNF) + pump (releasing 1 μg (about 40 pMol), 12 μl BDNF per day)
4) TrkB Agonist (low concentration) (N = 8): C7 avulsion + gelfoam (with 5 μg TrkB-agoAb4B19) + pump (releasing TrkB-agoAb4B19 1 μg (about 6.7 pMol), 12 μl per day)
5) TrkB Agonist (high concentration) (N = 8): C7 avulsion + gelfoam (with 5 μg TrkB-agoAb4B19) + pump (releasing TrkB-agoAb4B19 6 μg (about 40 pMol), 12 μl per day)

After 2-week perfusion of these drugs, the rats were sacrificed and perfused with 4% PFA. Sectioning of ventral spinal cord C6-C8 was performed longitudinally at a thickness of 20 μm and all ventral slides were collected. Every forth section was used for Nissl staining. The number of motor neurons in the ipsilateral side were counted, and the summed numbers for each animal was obtained in a double-blind manner. Cells were regarded as motoneurons when 1) the cellular diameter was greater than 30um and less then 50um; 2) a clear nucleus was presented in the cell; 3) the cell was located in the ventral horn. The number of motoneurons in sham group was regarded as control. We then calculated the survival rate of motoneurons as the ratio of motoneuron number in the experimental groups to that in the control (sham) group. Every forth section was also used for co-staining of nNOS and p75. The number of nNOS positive was counted and summed up for each animal in a double-blind manner.

3. Results

3.1. Development of TrkB agonistic monoclonal antibodies

Using human TrkB extracellular domain (amino acid 1–430, TrkB-ECD) as the antigen, a series of mouse monoclonal antibodies were generated using a fast immunization protocol followed by hybridoma methods. To increase the diversity of antibodies, we also used the yeast display technique to generate several monoclonal antibodies of rabbit origin. Positive clones containing antibodies against TrkB-ECD were screened by analyzed by ELISA. Following, the NFAT assay, a high throughput assay depending on the TrkB-PLCγ-Ca^{2+}-Calcineurin-NFAT pathway (Groth and Mermelstein, 2003; Merkouris et al., 2018; Todd et al., 2014), was applied to examine the potency of TrkB activation induced by these antibodies. The critical path (go-nogo tree) for the whole screening and selection procedures was established to ensure highly efficient screening and characterization (Supplementary Fig. 1).

To search for antibodies that could be used not only in animal models but also for human clinical use, we used ELISA again to screen for antibodies that bind both human and rat TrkB-ECD. Among these double-positive clones, approximately 40 active clones were identified from secondary screening using the NFAT assay with the Cellsensor TrkB-NFAT-bla CHO-K1 cells. Representative monoclonal antibodies exhibited dose-response of TrkB activation with EC50 values ranging from 0.05 nM to 10 nM, while BDNF has an EC50 of 0.22 nM (Fig. 1A). The maximal activation response (Emax) of TrkB agonist antibodies elicited a 60–90% efficacy of BDNF-induced TrkB activation. Subsequently, we selected several TrkB agonistic antibodies (TrkB-agoAbs) with high efficacy (> 60%) for TrkB activation for further characterizations.

The Trk family contains several other members with similar protein sequences and structures as TrkB. As shown in the sequence comparison between extracellular domains of TrkB and those of TrkA and TrkC, the three genes exhibited a substantial sequence homology (Supplementary Fig. 3F). We validated during the screening process that the TrkB antibodies absolutely did not induce TrkA activation using the Cellsensor TrkA-NFAT-bla CHO-K1 cells (Supplementary Fig. 2A). We next examined the binding specificity of the TrkB-agoAbs to all Trks (TrkA, TrkB, and TrkC) using ELISA. All TrkB-agoAbs could bind to only TrkB, but not TrkA or TrkC (Fig. 1B). Further, immunostaining experiments showed that only TrkB-CHO cells, but not TrkA-CHO cells, were stained positively by the TrkB agonistic antibody Ab4B19 (Supplementary Fig. 2B). Moreover, we have used conditional TrkB knock-out mice in which the *trkB* gene has been deleted in hypothalamic nucleus DMH by AAV expressing Cre into the DMH. Ab4B19 could reliably stain most of neurons in the entire section (red) except those expressing Cre recombinase (green) (Supplementary Fig. S2C). Taken together, Ab4B19 shows a significantly high specificity for TrkB.

Binding affinity is one of the most important characteristics for an antibody drug. To determine the binding affinity of TrkB-agoAbs with TrkB, we quantified the equilibrium dissociation constant (KD) for some TrkB-agoAbs using the surface plasmon resonance (SPR) function of Biacore. The KD values of TrkB-agoAbs ranged from 10^{-9} to 10^{-12} M, indicating very high binding affinity between the antibodies and TrkB (Fig. 1C).

3.2. Unique features of TrkB-agoAbs

To determine whether TrkB-agoAbs can activate the tyrosine kinase of TrkB as BDNF, we used AlphaLISA (Eglen et al., 2008) to quantify the level of TrkB-Tyr515 phosphorylation. hTrkB-CHO cells stably expressing hTrkB were treated with different concentrations of BDNF or TrkB-agoAbs for 30 min and proteins were collected for examination of TrkB phosphorylation. The EC50 values for TrkB-Y515 phosphorylation were determined based on the dose-response curves of each antibody. hTrkB-CHO cells were treated with TrkB-agoAbs at their respective EC50 concentrations at various time points to determine the time-course response and half-lives ($T_{1/2}$) of TrkB activation (Fig. 2A). Interestingly, the $T_{1/2}$s of nearly all TrkB-agoAbs were longer than BDNF (Fig. 2A, right, Supplementary Fig. 5B, C), suggesting that the effects of TrkB-agoAbs are longer-lasting than those of BDNF in terms of TrkB-mediated biological functions.

Next, we determined whether TrkB-agoAbs compete with BDNF in TrkB binding. In the activity-competition experiment, a saturated concentration (4 nM) of BDNF to achieve maximal activation was maintained in the hTrkB-CHO cell culture together with serial dilutions of TrkB-agoAbs, ranging from 0.01 to 100 nM. Since BDNF elicits the highest level of TrkB phosphorylation among all TrkB agonists (Fig. 2A), any competitive binding of TrkB-agoAbs to TrkB receptor in the same cultured neurons would move the equilibrium to the level elicited by TrkB-agoAbs, namely decrease the level of TrkB phosphorylation. Therefore, when TrkB is fully activated by BDNF, addition of TrkB-agoAb at increasing concentrations could provide information on its pharmacological characteristics. A TrkB-agoAb is considered competitive with BDNF if its log concentration curve is going downward, alternatively, the TrkB-agoAb is non-competitive when the log

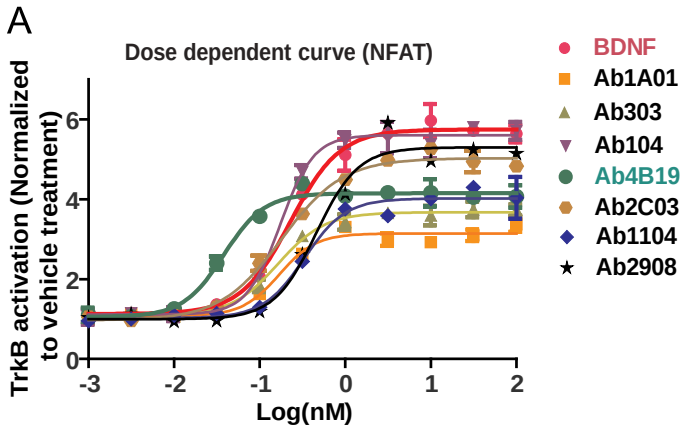

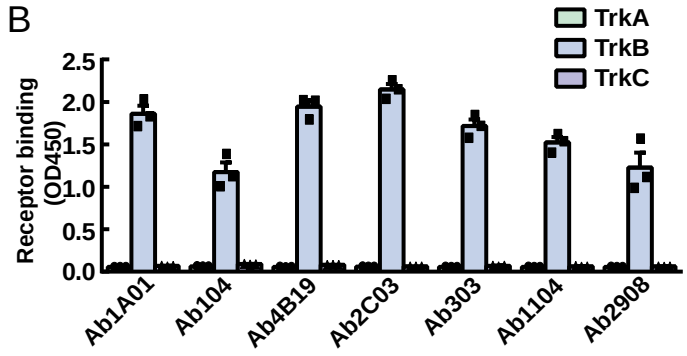

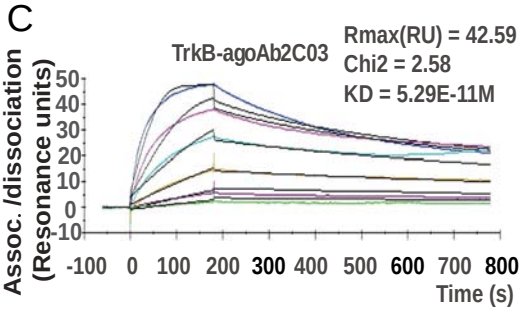

TrkB antibody	KD (M)
Ab1A01	5.57E-09
Ab104	6.68E-11
Ab4B19	<E-12
Ab2C03	5.29E-11
Ab303	4.02E-09
Ab1104	1.96E-10
Ab2908	2.2E-09

Fig. 1. Potency, specificity and affinity of TrkB agonistic antibodies (TrkB-agoAbs). (A) Dose-dependent activation of TrkB by different TrkB-agoAbs. TrkB activation was measured by NFAT assay in hTrkB-CHO cells treated with BDNF or TrkB-agoAbs for 4 h. The responses of these TrkB-agoAbs were normalized to that of vehicle treatment. In this and all the other figures, the data are presented as mean ± SEM. For this and all the other 96-well plate experiments, $n = 3$ wells, and each experiment was repeated for at least 2 times. (B) ELISA analysis showing that TrkB-agoAbs bind with only TrkB, but not TrkA or TrkC. Different TrkB-agoAbs (100 μl, 1 nM) were added to plates coated with 0.1 μg TrkA, TrkB or TrkC, respectively, and incubated overnight before adding HRP labeled secondary antibody. After removing excessive 2nd antibody, chromogenic substrate was added and absorbance at 450 nm (OD450) was read by Microplate Reader and represents the binding strength. (C) Biacore analysis of the affinities of various TrkB-agoAbs, with the antibodies as the stationary phase and antigen as the mobile phase. The left panel shows the associative and dissociative curves of a representative antibody. Antigen-antibody binding status was represented by the amount of resonance unit (RU) measured by Biacore system. The right panel shows the KD values of various antibodies.

concentration curve is straight. An upward curve, however, would suggest that the TrkB agonistic antibody has an additive effect with BDNF. Indeed, some TrkB-agoAbs were weakly competitive (*e.g.* red declining curves) while others were non-competitive (*e.g.* blue straight curves) with BDNF (Fig. 2B). Unexpectedly, we identified several TrkB-agoAbs with upward log concentration curves, suggesting that these antibodies exhibit additive effects with BDNF (green curves, Ab4B19 and Ab303) on TrkB activation (Fig. 2B).

Since some TrkB-agoAbs and BDNF worked additively on TrkB phosphorylation, we hypothesized that these antibodies may bind to regions on TrkB ECD that are different from BDNF. To examine this possibility, a series of plasmids with different versions of truncated TrkB were constructed to analyze the binding domains of the TrkB agonistic antibodies (Fig. 2C). The binding status of TrkB-agoAb with each truncated version of TrkB-ECD was determined using immunoprecipitation. Different TrkB-agoAbs exhibited different binding capacities to these truncated TrkB proteins (Fig. 2D). For example, Ab303 could only pull down full length (FL) and Δ2 TrkB, suggesting D3 is necessary for Ab303-TrkB binding (Supplementary Fig. 3A). Ab2C03 was able to bind all truncated TrkBs except Δ5, suggesting that it interacted with TrkB-D5, the region that BDNF binds to (Supplementary Fig. 3B). By comparison, the binding capacity of Ab4B19 was lost as long as the TrkB-D1 domain was deleted, suggesting that Ab4B19 is a D1-binding TrkB agonist (Fig. 2E). To further validate D1 is sufficient in TrkB binding by Ab4B19, a serials of constructs for TrkB extracellular domains, including TrkB-ECD, D1–3, D4–5, D1, D2, D3, were made to examine the binding capacity of Ab4B19 to TrkB-D1 (Supplementary Fig. 3C). We found Ab4B19 binds to D1–3 but not D4–5, and furthermore, Ab4B19 binds to D1 but not D2 or D3 (Supplementary Fig. 3D). Using similar approaches, we have identified antibodies that activated TrkB through binding to D3, and even juxtamembrane domain (data not shown). These results provide evidence for the first time that binding to a region remote from the BDNF-binding domain on TrkB extracellular region by antibody agonists could also achieve TrkB activation.

To select a pre-candidate agonistic antibody for further biological studies, we considered several characteristics including EC50, signaling characteristics, affinity, $T_{1/2}$ and competitiveness, as well as the capability of activating mouse/rat TrkB. Among all the TrkB-agoAbs, Ab4B19, a rabbit monoclonal antibody, had excellent EC50 value, high binding affinity and specificity and also exhibited potential additive effect with BDNF. Ab4B19 was therefore selected for further functional studies.

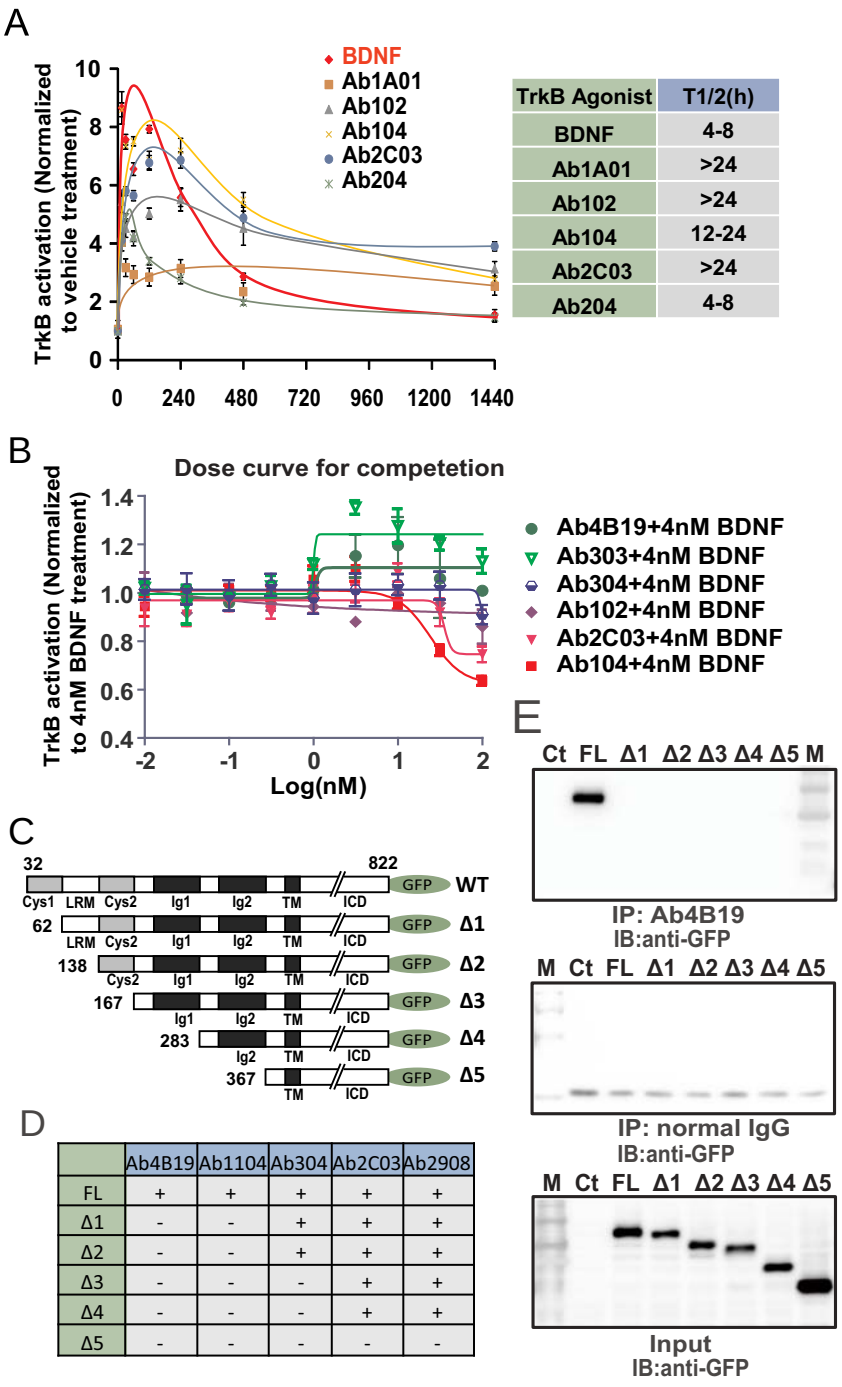

TrkB Agonist	T1/2(h)
BDNF	4-8
Ab1A01	>24
Ab102	>24
Ab104	12-24
Ab2C03	>24
Ab204	4-8

	Ab4B19	Ab1104	Ab304	Ab2C03	Ab2908
FL	+	+	+	+	+
Δ1	-	-	+	+	+
Δ2	-	-	+	+	+
Δ3	-	-	-	+	+
Δ4	-	-	-	+	+
Δ5	-	-	-	-	-

Fig. 2. Unique features of TrkB-agoAbs. (A) Time-course of TrkB activation by different TrkB-agoAbs using AlphaLISA in hTrkB-CHO cells. TrkB-agoAbs (at EC50 concentrations) were used to treat hTrkB-CHO cells, and protein samples were at different time points to measure the levels of phosphorylation at TrkB-Tyr515 with AlphaLISA analysis. The responses of these TrkB-agoAbs were normalized to that of vehicle treatment. Note that except for Ab204, majority of the TrkB-agoAbs decayed much slower than BDNF, with $T_{1/2}$ in the range of 12–24 h or over 24 h. (B) Competition between BDNF and TrkB-agoAbs in TrkB activation. Increasing doses of TrkB-agoAbs were added to the cultured hTrkB-CHO cells together with a saturate concentration of BDNF (4 nM), and TrkB activation was measured by AlphaLISA. The effects of 6 representative TrkB-agoAbs on the level of TrkB phosphorylation, normalized to that of BDNF, are presented. Two curves (red) declined with the increasing concentrations of the antibodies suggesting a direct competition between BDNF and these two TrkB-agoAbs (Ab2C03, Ab104), whereas two lines (blue) were straight indicating non-competitive nature of the two TrkB-agoAbs (Ab304, Ab102) with BDNF. Two upward curves (green) show that these two TrkB-agoAbs (Ab4B19, Ab303) could further increase TrkB activation even in the presence of saturated concentration of BDNF, suggesting a cooperative effect between the antibodies and BDNF. (C-E) Interaction of TrkB-agoAbs with different extracellular domains on TrkB. (C) A schematic diagram showing a series of truncated TrkB constructs used to analyze the binding domain of the Abs. (D) Binding capacity of different TrkB-agoAbs on different extracellular domains by Co-IP analysis using various truncated constructs of TrkB. (E) Immuno-precipitation showing that TrkB-D1 region is required for Ab4B19 binding of TrkB. The truncated plasmids shown in Fig. 2C were transfected into normal CHO cells respectively, and protein lysates were used for immunoprecipitation with different TrkB-agoAbs and detected by anti-GFP antibody. Normal IgG was used as the negative control. Note that Ab4B19-TrkB binding was lost when D1 region was deleted from TrkB. For this and all other qualitative measurements, independent experiments were repeated at least 3 times. (For interpretation of the references to colour in this figure legend, the reader is referred to the web version of this article.)

3.3. Comparison of signaling and functions between Ab4B19 and BDNF

We next examined whether Ab4B19 could activate TrkB and its downstream signaling events and eventually exhibit positive cellular functions. TrkB-CHO cells were treated with BDNF, Ab4B19, normal IgG (all 3 nM) or vehicle for 30 min, and TrkB (Y515) phosphorylation and downstream signaling events were analyzed by Western blotting. Similar to BDNF, Ab4B19 activated TrkB, triggered all major signaling pathways, and these effects were blocked by the pan inhibitor for Trk receptor tyrosine kinases, K252a (Fig. 3A–D). We also examined AbAB19 signaling in cultured cortical neurons and found Ab4B19 also activated TrkB and all downstream signals with a full-dose experiment (Han et al., 2019).

Both TrkB signal transduction and signal termination depend on endocytosis of TrkB after BDNF administration (Du et al., 2003; Reichardt, 2006). We examined the TrkB levels on the cell surface in a simplified time-course experiment using the classic biotinylation method. BDNF and Ab4B19 (both 3 nM) were added into DIV7 hippocampal neurons, and membrane protein biotinylations were performed at 0.25, 8 or 24 h after the administration of TrkB agonists. Biotinylated proteins and total proteins were collected respectively, and analyzed by Western blotting. Cell surface TrkB, pTrkB (Y515) and total TrkB all displayed a trend of decline over time (Fig. 3E). Remarkably, quantitative analyses show that Ab4B19 induced a slower or no decline of surface TrkB (Fig. 3F), a significantly less decrease in pTrkB 24 h after ligand application (Fig. 3G), and consistently far less reduction in total TrkB (Fig. 3H), compared with BDNF. Thus, it is possible that Ab4B19 (and some other TrkB-agoAbs) induces less TrkB endocytosis or triggers

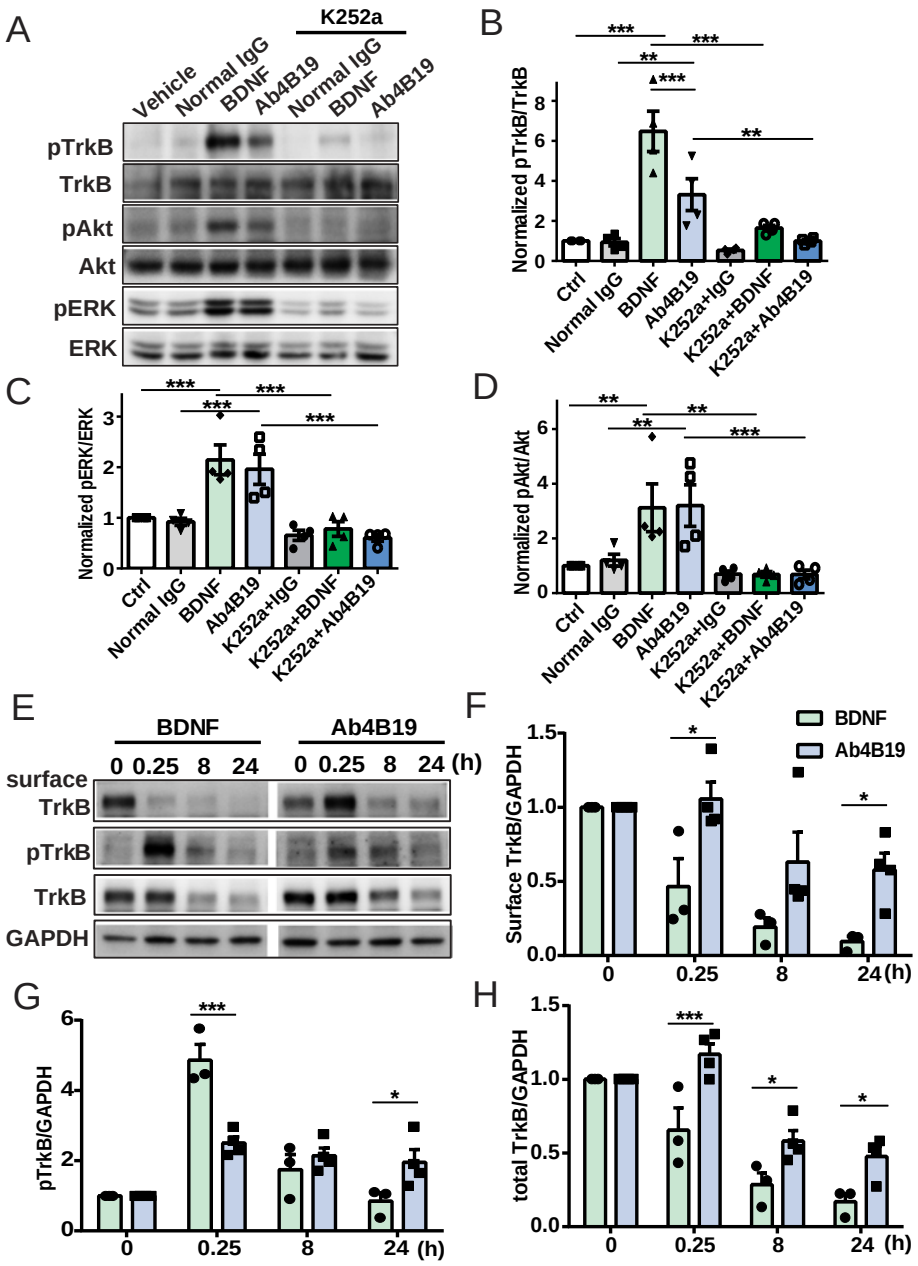

Fig. 3. Differential signaling of Ab4B19 and BDNF. (A) Activation of TrkB and its downstream signaling pathways by the antibody TrkB-agoAb4B19 in TrkB-CHO cell line. TrkB-CHO cells were treated with BDNF, TrkB-agoAb4B19, normal IgG (all at 3 nM) or vehicle for 30 min in the absence or presence of 300 nM K252a before cell lysis, followed by Western blotting. (B) Quantification of TrkB, Akt, and ERK phosphorylation levels (ratio to those of total proteins). The levels of vehicle treatment were normalized to 1. Statistical analyses were carried out using one-way ANOVA, followed by *post hoc* analysis. $^{*}P < .05$, $^{**}P < .01$, $^{***}P < .001$. (C) The change of surface TrkB, pTrkB and total TrkB over time after BDNF or Ab4B19 treatment. Hippocampal neurons (DIV7) were treated with 3 nM BDNF or Ab4B19, and biotinylated membrane proteins and total proteins were lysed, followed by Western blotting. Quantified analysis of surface TrkB (D), pTrkB (E), and total TrkB (F) were done. Statistical analyses were carried out using two-way ANOVA, $^{*}P < .05$, $^{***}P < .001$, all the experiments in this figure were repeated at least three times with independent cultures.

more TrkB recycling, resulting in far less TrkB degradation upon ligand treatment. Regardless, these results reveal another feature of Ab4B19 superior to BDNF, and explain the longer lasting TrkB kinetics of many of the TrkB-agoAbs (Fig. 2A, Supplementary Fig. 5B, C).

Two major cellular functions of BDNF are enhancing cell survival and promoting neurite outgrowth (Huang and Reichardt, 2003; Reichardt, 2006). Here, primary mouse cortical neurons and hTrkB-expressing PC12 cells were used to conduct the neurite outgrowth and cell survival assays, respectively. In mouse cortical neurons, Ab4B19 (0.3 and 1 nM) was applied to the cultures on DIV5 (5 days *in vitro*). Analysis of images from DIV10 cultures revealed that Ab4B19 treatment significantly increased the total length of neurites, number of extremities, and nodes (neurite branching points) per neuron at both 0.3 and 1 nM (Fig. 4A, B).

For cell survival assay, PC12 cells expressing human TrkB were deprived of serum to induce cell death. Cells were treated with BDNF or Ab4B19, and their protective effects were examined after the cells were starved for 16 h. Cell death was quantified by the ratio of the number of caspase 3 positive cells to total number of cells. Ab4B19 elicited a dose-dependent enhancement of cell survival, with EC50 at 0.004 nM (Fig. 4C). The survival effect was completely blocked by two different Trk inhibitors K252a and AZD-1332 (Fig. 4C). The Caspase-3 activity was shown by a fluorescent substrate of activated Caspase-3 (Fig. 4D), and the cell number was adjusted to a similar level (Supplementary Fig. 4A). In contrast, neither BDNF nor Ab4B19 could rescue serum-deprived normal PC12 cells, which only express TrkA and was protected by NGF (Supplementary Fig. 4B). Furthermore, Ab4B19 also shows universal survival effects on cultured mouse neurons and human embryonic stem cells (hESC)-derived neurons as BDNF (see Han et al., 2019).

3.4. Pharmacological properties of Ab4B19 superior to BDNF

Treatment of ALS with recombinant BDNF protein failed in clinical trials because of several intrinsic limitations, including BDNF's poor diffusibility, instability and activation of both TrkB and $p75^{NTR}$

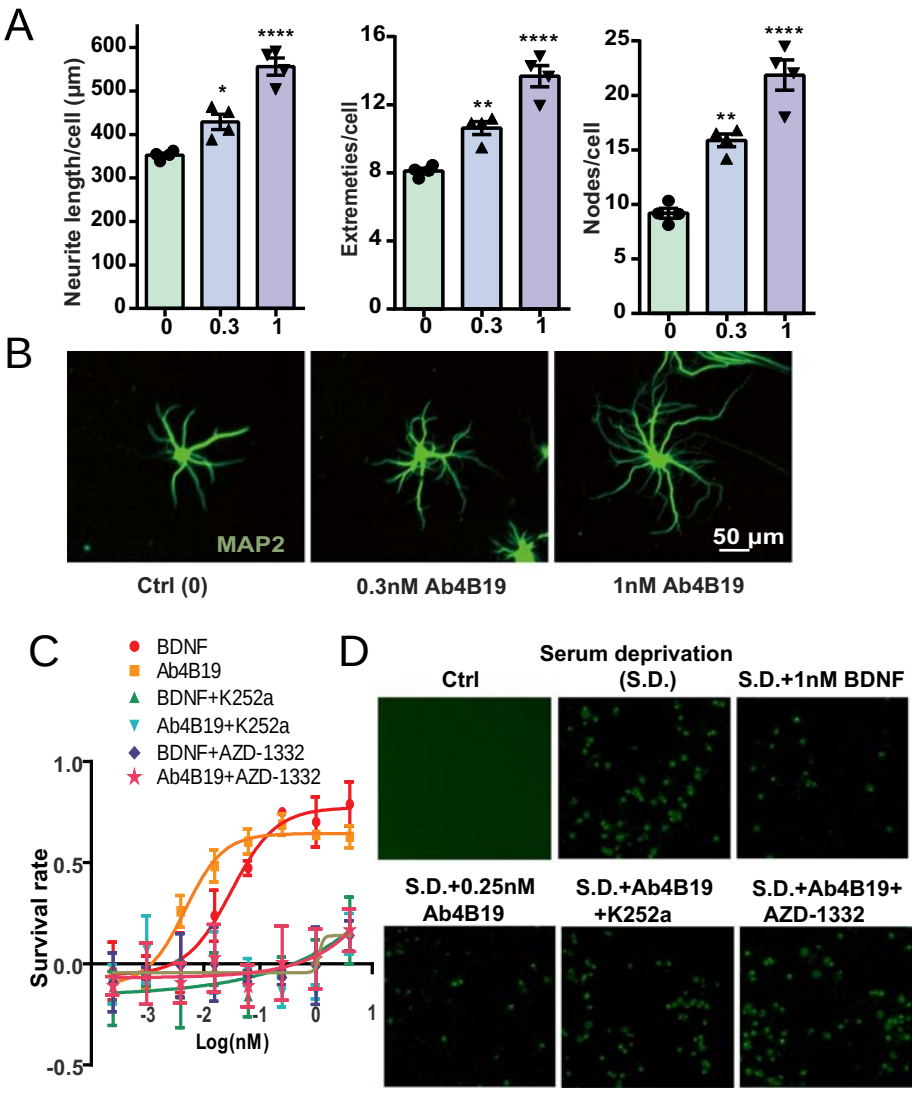

Fig. 4. Cellular functions of Ab4B19. (A) Effect of Ab4B19 on neurite outgrowth. Primary neurons (DIV5) from E17 mouse cortex were treated with Ab4B19 in culture for 5 days, stained with antibody against the dendritic marker MAP2, and the dendritic processes were quantified. The increases in total neurite lengths, extremities and nodes per cell by Ab4B19 at different concentrations (0.3 and 1 nM, respectively) are shown. Statistical analyses were carried out using one-way ANOVA, $^{*}P < .05$, $^{**}P < .01$, $^{***}P < .001$). The experiment was repeated four times with independent cultures. (B) Immunofluorescence images of neuronal soma and dendrites. (C) Effect of Ab4B19 on neuronal survival. Different doses of BDNF or Ab4B19 were applied to serum-deprived cultures of hTrkB-PC12 cells in the absence or presence of Trk inhibitors (300 nM K252a or 50 nM AZD-1332), and the cell apoptotic levels were determined by the ratio of the number of caspase 3 positive cells to total number of cells, using a caspase 3-substrate kit. Survival rates were determined by the decreased apoptotic levels normalized to that of vehicle treatment. Note that the EC50 of Ab4B19 is 0.004 nM, even lower than that of BDNF (0.03 nM). (D) Immunofluorescence images of caspase3 activity under different treatment conditions.

(Henriques et al., 2010). Except for the high affinity receptor TrkB, BDNF also stimulates the low-affinity $p75^{NTR}$ that mediates apoptotic signaling (Frade et al., 1996). However, Ab4B19 was found to bind selectively to TrkB but not $p75^{NTR}$ (Fig. 5A). Activation of $p75^{NTR}$ by cognate ligands induced transient separation of its death domains, which can be detected as large oscillations in real-time homo-FRET anisotropy measurements (Vilar et al., 2009). To further characterize the differences in signaling mediated by BDNF and Ab4B19, we used this assay to measure $p75^{NTR}$ activation. We found that in contrast to BDNF (Fig. 5B, lower), TrkB-agoAb4B19 did not induce any $p75^{NTR}$ -mediated oscillation (Fig. 5B, upper). These results together indicate that one significant advantage of Ab4B19 over BDNF is that it does not bind or activate $p75^{NTR}$.

BDNF is a highly charged molecule with pI of approximately 10 (Leibrock et al., 1989), which hinders its diffusion in target tissues (Croll et al., 1998). To test whether Ab4B19 overcomes this problem, we injected FITC-labeled BDNF or Ab4B19 (5 μg in 5 μl) into the L2-L3 lumbar of the rat spinal cord and examined their distributions 24 h later. We used equal mass concentration (5 μg in 5 μl) to compare the diffusion of BDNF or Ab4B19, because they should have similar fluorescent intensity. Here, it should be noted that BDNF and 4B19 were used in equal mass but not equal mole, because proteins in equal mass have approximately equal numbers of -NH2, the chemical group used for FITC conjunction. To ensure the amount of FITC-labeled BDNF and that of FITC-labeled Ab4B19 immediately before the injection were the same. We compared the fluorescent intensities of these two FITC-labeled proteins in a serial dilution. Very similar levels of fluorescence are seen for these two proteins at different dilutions (Supplementary Fig. 4C). Serial sections were collected starting from the injection site and sections at 0 μm, 300 μm, 600 μm, 1.2 mm and 3 mm were imaged (Fig. 5C). There were notable signals of FITC-labeled Ab4B19 in the motoneuron area of the spinal cord even 3 mm away from the injection site (Fig. 5D). In contrast, signals of FITC-labeled BDNF were merely restricted in the injection site (Fig. 5D). Thus, Ab4B19 is much more diffusible in nerve tissues than BDNF.

BDNF is rather unstable when exposed to 37 °C or even room temperature, and thus has poor pharmacokinetic features (Poduslo and Curran, 1996; Sakane and Pardridge, 1997). Antibodies, especially IgGs, have longer half-lives due to the unique protection through FcRn, which reduces lysosomal degradation and recycles antibodies to cell surface (Roopenian and Akilesh, 2007). To determine the pharmacokinetics of Ab4B19 in mice, 3 mg/kg body weight of Ab4B19 was injected through the tail vein. Blood and brain tissue samples were collected at different time points and stored at −80 °C immediately thereafter. The levels of Ab4B19 were analyzed with ELISA and the time-course curve was plotted. The $T_{1/2}$ for the rabbit antibody Ab4B19 was approximately 3 days in the blood and 5 days in brain tissues in mice (Fig. 5E). In comparison, the $T_{1/2}$ of BDNF is about several minutes in mice blood (Poduslo and Curran, 1996; Sakane and Pardridge, 1997). These results suggest that Ab4B19 is far more superior to BDNF

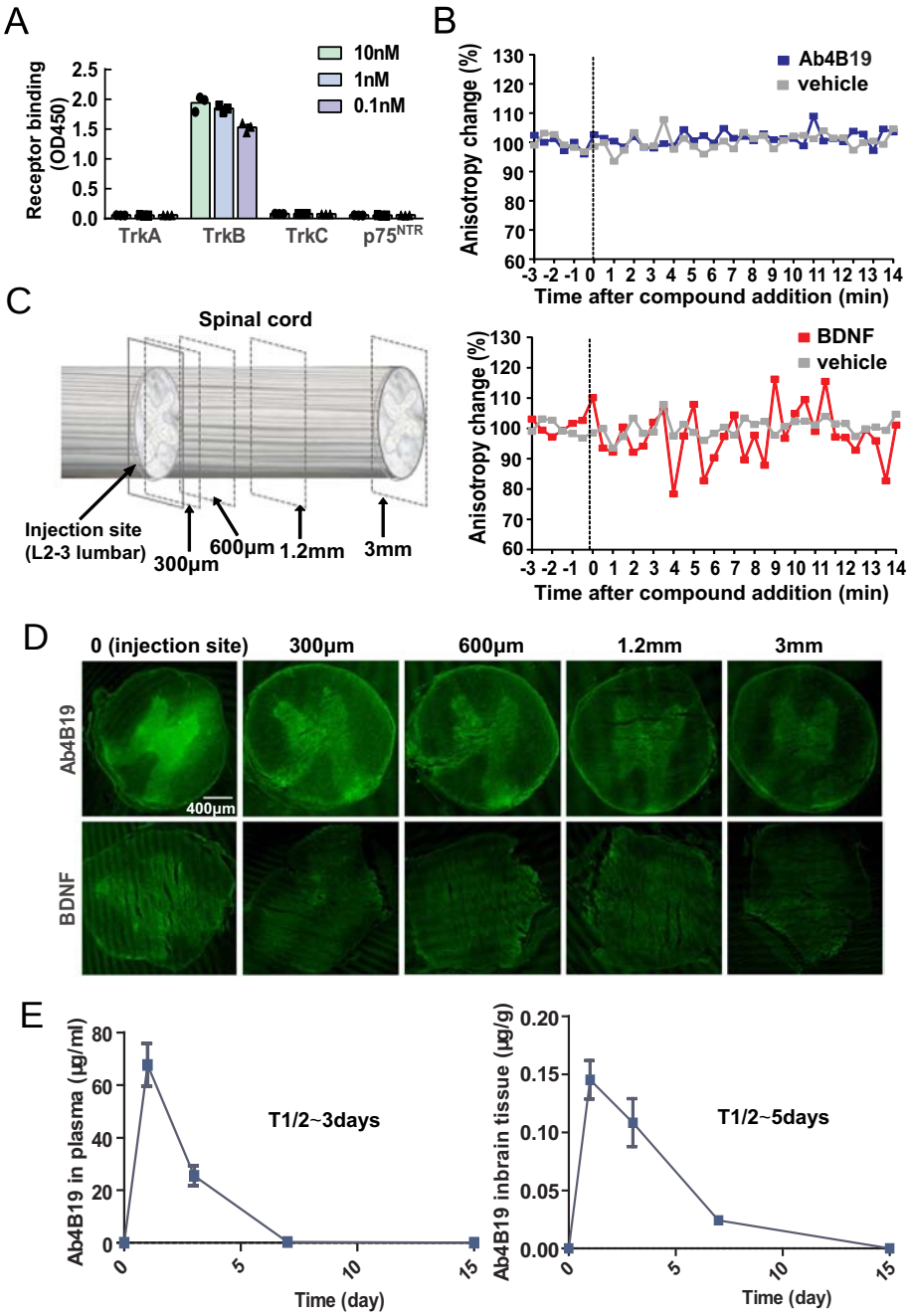

Fig. 5. Pharmacological properties of Ab4B19 superior to BDNF. (A) ELISA analysis showing that Ab4B19 was able to bind to only TrkB but not TrkA, TrkC or P75. Same method as in Fig. 1B was applied with 0.1, 1 and 10 nM Ab4B19. (B) Live cell homo-FRET anisotropy of $p75^{NTR}$ in COS cells in response to Ab4B19 and BDNF. Left panel shows representative traces of average anisotropy changes after addition of TrkB-agoAb4B19 (3 nM at 0 min) or vehicle (PBS) in cells expressing wild-type rat $p75^{NTR}$, whereas right panel shows representative traces of average anisotropy change after addition of BDNF (3 nM at 0 min) or vehicle (PBS). (C, D) Schematic diagram (C) and fluorescence imaging (D) of diffusion of FITC-labeled Ab4B19 and BDNF in the spinal cord. FITC-labeled TrkB agonists (both BDNF and Ab4B19, 5 μg in 5 μl) were injected into the L2-L3 lumbar of spinal cords, isolated 24 h later, processed and imaged at 0 μm, 300 μm, 600 μm, 1.2 mm and 3 mm from the injection site. (E) The pharmacokinetic curves of Ab4B19 in plasma (left) and brain tissues (right) of mice. Ab4B19 was injected through the tail vein of mice ($n = 4$). Plasma and brain tissues were collected at indicated time points for Ab4B19 quantification by ELISA.

in terms of pharmacokinetics.

3.5. Inhibition of cell death in cultured motoneurons

To evaluate the therapeutic potential of Ab4B19 in motoneuron degenerative diseases, we used an *in vitro* model to investigate the efficacy of Ab4B19 on motoneurons. Cultured motoneurons were positively stained with a pan-neuronal marker, beta III Tubulin (Tuj1) and a cholinergic neuron specific marker, choline acetyltransferase (ChAT) at DIV4 (Supplementary Fig. 5A). While a small number of Hoechst-labeled cells were ChAT negative (arrows in Supplementary Fig. 5A), the majority of Tuj1 cells were also stained with ChAT. It was estimated that > 90% of the cultured cells were ChAT-positive motoneurons.

We first analyzed the signaling events induced by BDNF and Ab4B19. Cultured motoneurons were treated with Ab4B19 at various concentrations for either 15 or 30 min, in parallel with BDNF (1 nM). The phosphorylation of TrkB and its downstream kinases, Akt1 and Erk1/2, were elevated by Ab4B19 in a dose-dependent manner (Fig. 6A). Compared with BDNF, Ab4B19 elicited a slightly lower but more sustained activation of TrkB and its downstream signaling events. At 24 h post treatment, pTrkB remained at a higher level in neurons treated with Ab4B19 as compared to those treated with BDNF (Supplementary Fig. 5B, C).

Serum deprivation induces motoneuron death *in vitro* (Wiese et al., 2010). In motoneurons cultured in complete medium for 3 days (DIV3), and then switched to serum-free medium containing BDNF (2 nM), Ab4B19 (3 nM) or horse serum and cell viability was assessed 24 h later. Apoptosis was determined by transferase-mediated deoxyuridine triphosphate-biotin nick end labeling (TUNEL) assay. Consistent with previous reports, serum deprivation led to marked cell loss and elevated apoptosis (Fig. 6B). More TUNEL-labeled cells were detected in the serum-deprived group compared to the control (Fig. 6B, 2nd row). In

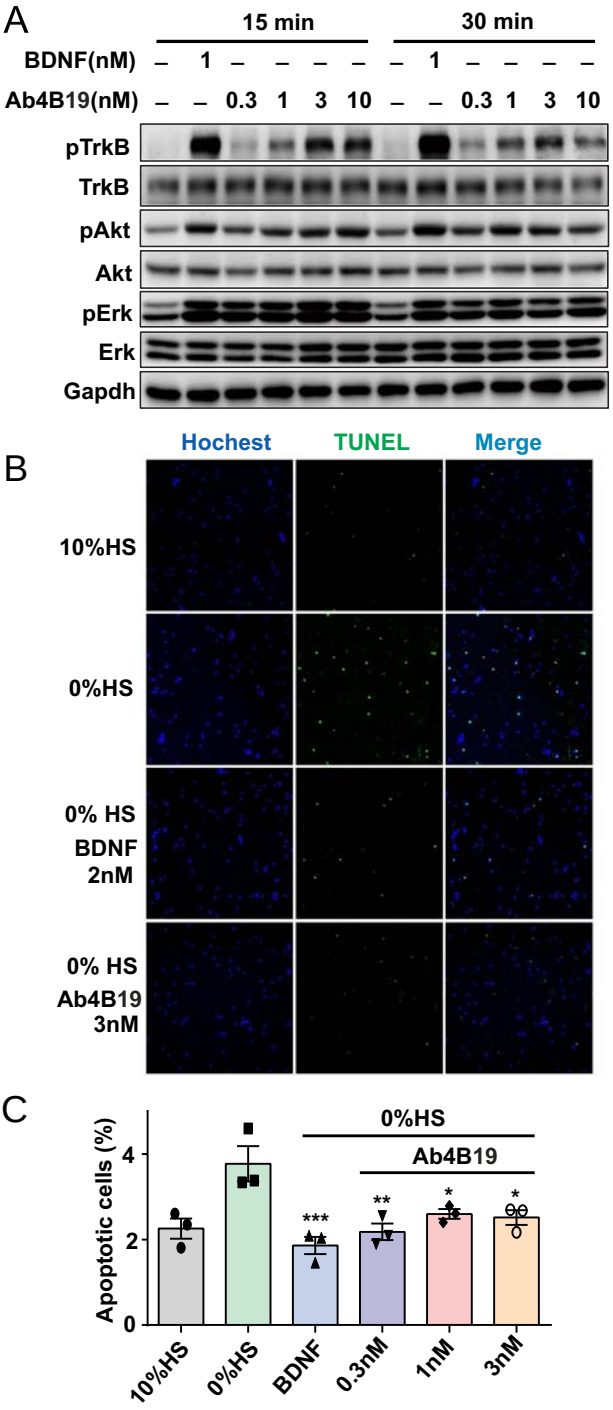

Fig. 6. TrkB activation and pro-survival functions of Ab4B19 in primary mouse motoneurons. (A) TrkB signaling pathways activated by Ab4B19 (0.3, 1, 3 and 10 nM) and BDNF (1 nM) at 15 and 30 min, analyzed by Western Blotting. (B) Reduction of motoneuron apoptosis by Ab4B19. Motoneurons were cultured for 3 days and then switched to serum-deprivation conditions for 24 h in the presence of BDNF (2 nM) or Ab4B19 (3 nM). Apoptotic neurons were measured by TUNEL assay (green). Nuclei were stained with Hoechst (blue). (C) Quantification of cell apoptosis as measured by percentage of TUNEL positive cells. BDNF and all doses of Ab4B19 significantly reduced cell apoptosis induced by serum-deprivation. ($n = 3$ cultures in each condition, Statistical analyses were carried out using one-way ANOVA, $^{*}P < .05$, $^{**}P < .01$). (For interpretation of the references to colour in this figure legend, the reader is referred to the web version of this article.)

cultures treated with BDNF or Ab4B19, the number of TUNEL-labeled cells was markedly reduced (Fig. 6B, 3rd and 4th rows). Quantitative analysis revealed a significant reduction in the number of apoptotic neurons after treatment with BDNF or Ab4B19 at a concentration as low as 0.3 nM (Fig. 6C). These results indicate that Ab4B19 is as effective as BDNF in attenuating motoneuron death in culture.

3.6. Attenuation of motoneuron degeneration by Ab4B19 in the spinal avulsion model

To investigate the effect of Ab4B19 in motoneuron degeneration *in vivo*, we used a well-established spinal root avulsion model to induce motoneuron damage (Kishino et al., 1997), because it is easy to control the onset of cell death (the time of avulsion). BDNF has been shown to rescue motoneuron death in this model (Kishino et al., 1997; Wu et al., 2003), and therefore was used as a positive control. Following an established protocol, a gelfoam soaked with 200 pmol (5 μg) BDNF were gently placed onto the injured C7 spinal cord surface after spinal root avulsion. To overcome its limitation of short half-life, BDNF was continuously delivered through osmotic mini-pump (40 pmol/day) for two weeks. While only 30.7% of motoneurons remained alive in avulsed animals, treatment with BDNF resulted in 77.2% of neuronal survival. In comparison, Ab4B19 administrated at low (6.7 pmol/day) and high (40 pmol/day) concentrations also attenuated motoneuron death, resulting in 76.2% and 80.9% survival of motoneurons, respectively (Fig. 7F). In addition, in BDNF and Ab4B19-treated motoneurons, healthy subcellular architectures, including big nuclei, dark stained rough endoplasmic reticulum and big cytoplasm, were observed in Nissl stained sections (Fig. 7A, C, D and E). By contrast, abnormal cellular appearances were observed in PBS-treated cells, without recognizable subcellular structures (Fig. 7B). A few motoneurons from BDNF and Ab4B19-treated groups exhibited hypertrophy, although these morphological changes were difficult to quantify.

Neuronal nitric oxide synthase (nNOS) has been shown to be upregulated in avulsed motoneurons from the first week after injury, and the increased levels of nNOS are maintained for weeks (Wu et al., 1994). These nNOS-positive cells eventually die as disease progresses (Sasaki et al., 2001). Although it remains unclear whether the increase in nNOS is the cause or consequence of neuronal death, the product of nNOS-mediated reaction, nitric oxide (NO), was reported to be coupled with necrosis and apoptosis (Brown, 2010). Many nNOS-positive motoneurons were observed in the ipsilateral, but not contralateral spinal cord of PBS-treated avulsed animals. In the Ab4B19- and BDNF-treated animals, very few nNOS-positive cells were observed (Fig. 8A). Quantitative analysis revealed that the number of nNOS-positive cells per section of spinal cord were reduced by > 5 fold in the BDNF- and Ab4B19 treated groups in a double-blind manner, compared with the PBS control (Fig. 8B). Taken together, the TrkB agonist antibody is a potent inhibitor of injury-induced motoneuron loss *in vivo*.

As the low-affinity receptor of BDNF, $p75^{NTR}$ is implicated in cell death, and neurons undergoing apoptosis often exhibit an increase in $p75^{NTR}$ expression (Ibáñez and Simi, 2012; Nykjaer et al., 2005). Some spinal cord cells express basal levels of $p75^{NTR}$, and avulsion increased the number of $p75^{NTR}$-positive cells in the PBS group (Fig. 8A. See also (Roberson et al., 1995; Wu, 1996)). Interestingly, after unblinding of nNOS positive cell counting, we found BDNF treatment also elevated $p75^{NTR}$ expression, as reflected by the increased number of $p75^{NTR}$-positive cells and the intense $p75^{NTR}$-immunoreactivity in representative cells from a fraction of the randomly taken p75-staining images (Fig. 8A, arrowheads, third image, middle row). Unlike that induced by BDNF, however, treatment by Ab4B19 had a less number of $p75^{NTR}$-positive cells (Fig. 8A, arrowheads). Although we could not count $p75^{NTR}$-positive cells using the same rigorous method mentioned above, all sections of $p75^{NTR}$-immuno-stained serial sections from two rats were fully examined. We found obvious difference between these two groups (Supplementary Fig. 6). These results raised the possibility

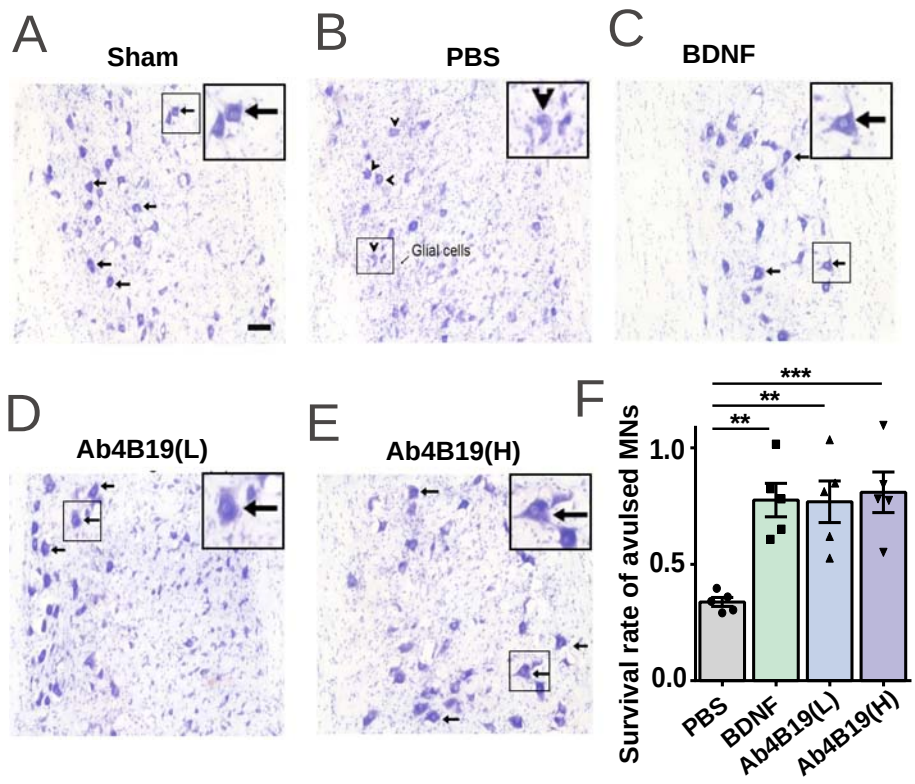

Fig. 7. Prevention of motoneuron degeneration by Ab4B19 in the rat spinal avulsion model. (A–E) Nissl stained longitudinal sections of avulsed spinal cords under various treatment conditions. Rats were assigned to sham, PBS, BDNF, Ab4B19 (low concentration, L, 6.7 pmol/day) and Ab4B19 (high concentration, H, 40 pmol/day) treatment groups and sacrificed for analysis on day 14 post surgery. Arrows indicate the motoneurons with healthy morphology and arrowheads in (B) indicate cells with dying cell morphology. (F) Quantification of motoneuron survival expressed as the ratio of the number of motoneurons in avulsed groups to that from the sham control. (n = 5 rats in each condition. Statistical analyses were carried out using one-way ANOVA, *P < .05, **P < .01, ***P < .001. Scale bar in A indicates 100 μm).

that BDNF, through interaction with p75^{NTR}, may also promote cell death, a potential aversive effect that cannot be ignored. Interestingly, while most of the p75^{NTR}-positive cells in PBS-treated animals were co-stained with nNOS (Fig. 8A, arrow), p75^{NTR}-positive cells in the BDNF-treated group were not co-stained by nNOS (Fig. 8A). While the significance of these findings is unclear, these results suggest that unlike Ab4B19 which specifically activates TrkB to inhibit neuronal death, BDNF may additionally induce non-physiological changes by activating the p75^{NTR} signaling.

4. Discussion

While the BDNF-TrkB signaling pathway has long been recognized as a potential drug target for nervous system disorders, decades of efforts by academia and industry have so far yield no success in the clinic (Lu et al., 2013). BDNF itself has been proved to be not a druggable molecule, due to its poor PK, stickiness, as well as its dual activation of TrkB and p75^{NTR} (Lu et al., 2013; Morse et al., 1993; Nagahara and Tuszynski, 2011; Poduslo and Curran, 1996). Although a number of TrkB activating antibodies have been generated (Merkouris et al., 2018; Qian et al., 2006; Todd et al., 2014; Traub et al., 2017), none has been shown to be superior to BDNF. In this study, we screened and characterized a large number of TrkB antibodies, and searched for drug-like TrkB-agoAbs with unique properties that make them more suitable for therapeutic applications. Through multiple assays, we identified Ab4B19 as one of the lead antibodies that were able to bind TrkB with high affinity and specificity, and exhibited similar signaling transduction and biological functions as BDNF. Compared with BDNF, Ab4B19 interacted with TrkB in a distinct domain, activated TrkB with a much longer duration, exhibited a slower endocytosis and reduced intracellular degradation of TrkB, and worked additively with endogenous BDNF. Further, unlike BDNF, administration of Ab4B19 elicited no increase the expression of p75^{NTR} in the spinal cord avulsion model *in vivo*, eliminating the concern for p75^{NTR}-mediated cell death.

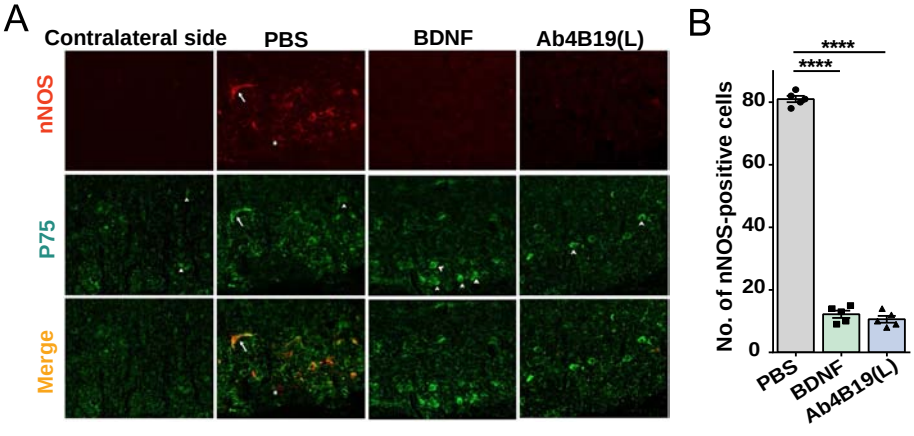

Fig. 8. Reduction of nNOS-positive cells by Ab4B19 in the rat spinal avulsion model. (A) Representative images of the spinal cord sections after BDNF or Ab4B19 treatment. Arrowheads indicate p75^{NTR} -positive cells, whereas arrows point to cells that are both nNOS- and p75^{NTR} -positive. Both BDNF- and Ab4B19- treated groups show fewer nNOS-positive cells, compared with the PBS treated group. Note that there are more p75^{NTR} -positive cells in the BDNF-treated group, but not in Ab4B19-treated groups. The PBS treated group exhibit more cells doubly stained with nNOS and p75^{NTR}. (B) Quantification of the number of nNOS-positive cells under various treatment conditions. (n = 5 rats for each group, ****p < .0001, chi-square test).

More importantly, Ab4B19 penetrated into and readily diffused in brain tissues (see Han et al., 2019.), and had a blood half-life more than hundreds of times that of BDNF. We also showed that Ab4B19 exhibited its therapeutic efficacy in both *in vitro* and *in vivo* models of motoneuron injury in the spinal cord. Therefore, Ab4B19 provides a tool to re-evaluate BDNF-based neurotrophic therapy for the treatment of motoneuron diseases and potentially other neurological disorders and some neuropsychiatric disorders (Autry and Monteggia, 2012).

For motoneuron degeneration, the rationale for a BDNF-based therapy is quite strong. BDNF enhances survival, and promotes dendritic and axon growth of motoneurons (Henriques et al., 2010). In animal models of axotomy induced motoneuron degeneration, BDNF could be retrogradely transported in motor neurons (Yan et al., 1992), and prevent motoneuron death in the axotomy model of neonatal rats (Sendtner et al., 1992; Yan et al., 1992). More importantly, in the rat spinal root avulsion model, BDNF infusion with the osmotic minipump elicited protective effects on motoneuron death, soma atrophy and choline acetyl transferase (ChAT) reduction when delivered intrathecally immediately after avulsion or even delivered after a two-week delay (Kishino et al., 1997). There is also evidence for a role of BDNF in ALS treatment. Earlier reports showed that in the spinal cord of ALS patients, TrkB mRNA and protein levels were elevated but the TrkB proteins were less phosphorylated (Mutoh et al., 2000). FUS, a pathogenic gene strongly associated with ALS, alters the expression and alternative splicing of BDNF (Lagier-Tourenne et al., 2012; Qiu et al., 2014), presumably contributing to the down-regulation of the levels of BDNF protein and TrkB phosphorylation seen in FUS mutant mice (Qiu et al., 2014). BDNF also facilitates functional recovery from neurodegenerative changes induced by CSF (cerebral spinal fluid) from ALS patient in motor neuron cell line (Shruthi et al., 2017). In marked contrast to the successes in preclinical studies on motoneuron degeneration, placebo-controlled ALS clinical trials using either peripheral systemic or intrathecal administrations of BDNF have all failed: no clinical benefits on survival or on the ALS functional rating scale (ALSFRS) score were observed (Neurology, 1999) (Ochs et al., 2000).

There are strong reasons to believe that failures in clinical applications of BDNF were due to its three intrinsic limitations. In this study, we have developed a TrkB agonistic antibody Ab4B19 that overcomes the major shortcomings of BDNF. First, BDNF has an extremely short half-life (minutes in blood and an hour in CSF) (Poduslo and Curran, 1996; Sakane and Pardridge, 1997) (Soderquist et al., 2009). PK analysis in mouse blood and brain by ELISA showed that Ab4B19 has a half-life of several days. To circumvent the problem of short half-life of BDNF, we added an osmotic mini-pump to continuously deliver BDNF to the avulsed spinal cord. One can imagine how impractical should this be used in the clinic. Second, the diffusion rate of BDNF is very low in tissues because of its strong positive charges. For example, unlike NGF, BDNF protein infused into the midbrain remained in the injection site without penetrating into the brain tissue (Croll et al., 1998; Morse et al., 1993). We showed in this study that FITC-labeled Ab4B19, but not BDNF, diffused extensively in the spinal tissues after spinal cord injection. Third, we found that in the spinal cord avulsion model, BDNF activates its low-affinity receptor, $p75^{NTR}$ (Figs. 5B, 8A) which mediates apoptotic signaling, cell death and possibly other actions (Chao, 1994; Hempstead, 2002). $P75^{NTR}$ was upregulated in SOD1 mice or ALS patients (Lowry et al., 2001; Shepheard et al., 2014). Application of a $p75^{NTR}$ antisense peptide or antagonist prevented cell death and slowed down the progression of ALS phenotypes in SOD-1 animals (Matusica et al., 2016; Turner et al., 2003; Turner et al., 2004). It is unclear whether activation of $p75^{NTR}$ in spinal neurons had contributed to the clinical failures. Regardless, the negative effects by $p75^{NTR}$ activation may counteract the benefits of BDNF through TrkB activation. We carefully examined the binding specificity of Ab4B19 with $p75^{NTR}$ and other Trks and confirmed that TrkB is the only member that Ab4B19 binds. The real-time homo-FRET anisotropy measurement showed that unlike BDNF, Ab4B19 does not induce $p75^{NTR}$ activation. The selective activation of TrkB but not $p75^{NTR}$, plus better PK and diffusibility, makes Ab4B19 a better drug candidate than BDNF itself for BDNF-based therapies.

TrkB agonistic antibodies have been developed before. For example, the antibody 29D7 (Qian et al., 2006) was reported to be beneficial in the treatment of cervical spinal cord injury (Fouad et al., 2010), optic nerve injury (Hu et al., 2010), neonatal hypoxia injury (Kim et al., 2014), and Huntingtin-expressed neurons (Todd et al., 2014) in rodent models. These studies have not addressed the issues of PK and $p75^{NTR}$ activation. Further, the $T_{1/2}$ of TrkB activation or the binding domain of 29D7 was not revealed. In a separate study, two TrkB antibodies 1D7 and 21G3 were found to bind TrkB, and rescue neuronal death in the retina in a glaucoma model (Bai et al., 2010). Again, it was unclear whether these antibodies were compared with BDNF in terms of EC50s, half-lives of pTrkB and $p75^{NTR}$ activation. Traub et al. identified two antibodies that appear to allosterically activate TrkB, but the potency of these two antibodies was much lower than BDNF (Traub et al., 2017). Recently, Merkouris et al. characterized a series of TrkB agonistic antibodies merely from a human short-chain variable fragment antibody library. These antibodies exhibited similar TrkB activating potency as BDNF and were competitive with BDNF in terms of TrkB binding (Merkouris et al., 2018).

In the present study, we have identified a TrkB agonistic antibody Ab4B19 with several unique features not described before. First, Ab4B19 induced a prolonged TrkB activation; the $T_{1/2}$ of TrkB phosphorylation was about 5 h for BDNF, but > 24 h for Ab4B19, suggesting that it has extended biological effects. Based on our current results and previous work (Guo et al., 2014; Ji et al., 2010), this prolonged TrkB activation is likely mediated by the slower antibody induced decline of cell-surface TrkB compared with BDNF. Second, we mapped Ab4B19 binding to the D1 domain on the TrkB extracellular region. This is different from most of the previously reported TrkB antibodies, which bind to D5 on TrkB, the same binding domain as BDNF. Therefore they are likely to be competitive with endogenous BDNF (Ultsch et al., 1999). Third, competition analysis revealed that in the presence of saturated amount of BDNF, Ab4B19 could still induce further TrkB activation, suggesting that it may work cooperatively rather than competitively with endogenous BDNF. Taken together, we have developed a TrkB agonistic antibody with certain advantages compared with other TrkB agonists.

Using the culture and the spinal cord avulsion models, the present study showed that treatment with Ab4B19 attenuated injury-induced motoneuron loss. We also found that treatment with BDNF, but not Ab4B19, induced an upregulation of $p75^{NTR}$, which is often associated with apoptosis in certain cells in the spinal cord. Upregulation of $p75^{NTR}$ is thought to contribute to pathophysiology of ALS (Lowry et al., 2001; Shepheard et al., 2014). Future work should identify whether the $p75^{NTR}$-positive cells in ALS spinal cord are neurons or glial cells, and which type of neurons if applicable. Regardless, unlike BDNF, Ab4B19 does not have the drawback of elevating $p75^{NTR}$. While we do not know whether Ab4B19 could be useful in treating human ALS at the present time, we showed that Ab4B19 has a significant pro-survival effect on human ES-derived neurons under oxygen-glucose deprivation (see Han et al., 2019). Furthermore, comprehensive analysis of TrkB-agoAb using additional preclinical ALS models in the future should help provide solid foundation in testing whether TrkB-agoAb could be used in treating motoneuron disease or ALS in the clinic.

An interesting point is that we and others have consistently observed that for both BDNF and TrkB mAbs, the EC50 for cell survival is much lower than that for TrkB phosphorylation in PC12 cell line and primary cultured neurons, suggesting that only minimum TrkB activation is needed for neuronal protection. It has been shown that EC50 of PI3K-Akt and MAPK activation by TrkB agonists were approximately 1/10 of TrkB (Boltaev et al., 2017). This means that only 10% TrkB activation is required for full activation of PI3K-Akt and MAPK pathway. Meanwhile, the amplitude of TrkB activation appears not to be critical

for selecting an agnostic antibody. For neural protection and survival, Ab4B19 induced similar magnitudes of PI3K-Akt and MAPK activation as BDNF at saturate concentration. Similar PI3K-Akt and MAPK activation (Fig. 3A–D), together with longer $T_{1/2}$ (Supplementary Fig. 5B, C), less TrkB internalization and degradation (Fig. 3E, F, H), and non-competitive to BDNF (Fig. 2B), forms a strong rationale for selecting 4B19 as the lead BDNF mimetic antibody.

A number of issues remain to be addressed in future studies. First, TrkB agonists may also bind the truncated TrkB-T1, which is thought to act as a dominant negative isoform for full-length TrkB function or regulates calcium signals in astrocytes or peripheral organs (Fenner, 2012). Interestingly, deletion of TrkB-T1 in SOD1 mice induced pro-survival effects on motoneuron (Yanpallewar et al., 2012). No study has been published so far that reported the effects of TrkB agonistic antibodies on TrkB-T1. Second, the present study demonstrated the survival effects of Ab4b19 on motoneuron cell body. It is unclear whether Ab4B19 could also counter the Wallerian (axonal) degeneration and rescue the deficits in retrograde axonal transport. Third, experimental data are lacking whether Ab4B19 itself could be endocytosed and retrogradely transported along the motor axons. Last but not least, we showed that Ab4B19 applied to cell culture induced a prolonged activation, a longer surface life and less degradation of TrkB, compared with BDNF. However, it remains to be determined whether Ab4B19 applied to the axonal terminals of motoneurons, or administrated systemically, could also elicit the differential effects. Regardless of the outcome, it will be interesting to determine whether Ab4B19 delivered to cell body or proximal axons would elicit sufficient therapeutic effects *in vivo*, even if the retrograde signaling of Ab4B19 were disrupted.

In summary, we have developed a TrkB agonistic antibody with high TrkB-activating potency, and high specificity and affinity. In both *in vitro* and *in vivo* motoneuron injury models, Ab4B19 exhibited pro-survival effects. Detailed analysis revealed that Ab4B19 is a potential therapeutic agent with drug-like properties superior to BDNF and previously reported TrkB agonists, and may be further developed for the treatment of motoneuron diseases as well as other neurological disorders.

Funding and disclosure

This work was supported by the National Natural Science Foundation of China (81501105, 31730034), the Ministry of Education (Thousand Talent Program) to BL, Shenzhen Science Technology and Innovation Commission (JCYJ20170411152419928 and GJHZ20170314151528005), and Beijing Municipal Science & Technology Commission (Z151100003915118).

Declaration of Competing Interest

BL, WG and HYao are co-inventors of the filed patents related to all TrkB-agoAbs.

Acknowledgments

WG and BL initiated the project and designed the study. WG managed all the experiments, conducted the experiments of antibody screening and characterization. KP and WG conducted the AlphaLISA assays. YC conducted the cultured motoneuron experiments. HLi, KP and WW conducted the spinal avulsion experiments and analyzed the data. FH conducted the neurite outgrowth experiments. SW and YX conducted the experiments of pharmacokinetics. HYao, WZ and YD conducted some of antibody manufacture and preliminary screening. DS and WG contribute to Biacore SPR analysis. HLiu and WG conducted the experiment of specificity. VL conducted the homo-FRET anisotropy experiments. YX, SW, JShao and DS contributed to the biochemical and Co-IP experiments. JShen, JShao and SW contributed to truncated constructs design. JShao and YD contributed to antigen and antibody purification. WG and BL wrote the manuscript. FH, YC, HLi, HYou and WW also contributed to the discussion and manuscript writing. Rabbit antibody manufacture with yeast display was done by a CRO company (Sino Biol.).

Appendix A. Supplementary data

Supplementary data to this article can be found online at https://doi.org/10.1016/j.nbd.2019.104590.

References

Autry, A.E., Monteggia, L.M., 2012. Brain-derived neurotrophic factor and neuropsychiatric disorders. Pharmacol. Rev. 64, 238.
Bai, Y., Xu, J., Brahimi, F., Zhuo, Y., Sarunic, M.V., Saragovi, H.U., 2010. An agonistic TrkB mAb causes sustained TrkB activation, delays RGC death, and protects the retinal structure in optic nerve Axotomy and in Glaucoma. Invest. Ophthalmol. Vis. Sci. 51, 4722–4731.
Boltaev, U., Meyer, Y., Tolibzoda, F., Jacques, T., Gassaway, M., Xu, Q., Wagner, F., Zhang, Y.-L., Palmer, M., Holson, E., et al., 2017. Multiplex quantitative assays indicate a need for reevaluating reported small-molecule TrkB agonists. Sci. Signal. 10.
Brown, G.C., 2010. Nitric oxide and neuronal death. Nitric Oxide 23, 153–165.
Camu, W., Henderson, C.E., 1992. Purification of embryonic rat motoneurons by panning on a monoclonal antibody to the low-affinity NGF receptor. Journal of Neuroscience Methods 44, 59–70.
Chao, M.V., 1994. The p75 neurotrophin receptor. J. Neurobiol. 25, 1373–1385.
Chao, M.V., 2003. Neurotrophins and their receptors: a convergence point for many signalling pathways. Nat. Rev. Neurosci. 4, 299–309.
Croll, S.D., Chesnutt, C.R., Rudge, J.S., Acheson, A., Ryan, T.E., Siuciak, J.A., DiStefano, P.S., Wiegand, S.J., Lindsay, R.M., 1998. Co-infusion with a TrkB-fc receptor body carrier enhances BDNF distribution in the adult rat brain. Exp. Neurol. 152, 20–33.
Dittrich, F., Ochs, G., GrosseWilde, A., Berweiler, U., Yan, Q., Miller, J.A., Toyka, K.V., Sendtner, M., 1996. Pharmacokinetics of intrathecally applied BDNF and effects on spinal motoneurons. Exp. Neurol. 141, 225–239.
Du, J., Feng, L., Zaitsev, E., Je, H.S., Liu, X.W., Lu, B., 2003. Regulation of TrkB receptor tyrosine kinase and its internalization by neuronal activity and Ca2+ influx. J. Cell Biol. 163, 385–395.
Eglen, R.M., Reisine, T., Roby, P., Rouleau, N., Illy, C., Bossé, R., Bielefeld, M., 2008. The use of AlphaScreen technology in HTS: current status. Curr. Chem. Genomics 1, 2–10.
Fenner, B.M., 2012. Truncated TrkB: beyond a dominant negative receptor. Cytokine Growth Factor Rev. 23, 15–24.
Fouad, D.K., Vavrek, R., Cho, D.S., 2010. A TrkB antibody agonist promotes plasticity following cervical spinal cord injury in adult rats. J. Neurotrauma 0 (null).
Frade, J.M., Rodriguez-Tebar, A., Barde, Y.A., 1996. Induction of cell death by endogenous nerve growth factor through its p75 receptor. Nature 383, 166–168.
Friedman, W.J., Greene, L.A., 1999. Neurotrophin signaling via Trks and p75. Exp. Cell Res. 253, 131–142.
Giehl, K.M., Tetzlaff, W., 1996. BDNF and NT-3, but not NGF, prevent axotomy-induced death of rat corticospinal neurons in vivo. Eur. J. Neurosci. 8, 1167–1175.
Gordon, P.H., 2013. Amyotrophic lateral sclerosis: an update for 2013 clinical features, pathophysiology, management and therapeutic trials. Aging Dis. 4, 295–310.
Graham, J.M., 2002. Isolation of a mouse motoneuron-enriched fraction from mouse spinal cord on a density barrier. ScientificWorldJournal 2, 1544–1546.
Greenberg, M.E., Xu, B., Lu, B., Hempstead, B.L., 2009. New insights in the biology of BDNF synthesis and release: implications in CNS function. J. Neurosci. 29, 12764–12767.
Groth, R.D., Mermelstein, P.G., 2003. Brain-derived neurotrophic factor activation of NFAT (nuclear factor of activated T-cells)-dependent transcription: a role for the transcription factor NFATc4 in neurotrophin-mediated gene expression. J. Neurosci. 23, 8125.
Gu, Y., Spasic, Z., Wu, W., 1997. The effects of remaining axons on motoneuron survival and NOS expression following Axotomy in the adult rat. Dev. Neurosci. 19, 255–259.
Guo, W., Ji, Y., Wang, S., Sun, Y., Lu, B., 2014. Neuronal activity alters BDNF–TrkB signaling kinetics and downstream functions. J. Cell Sci. 127, 2249–2260.
Han, F., Guan, X., Guo, W., Lu, B., 2019. Therapeutic potential of a TrkB agonistic antibody for ischemic brain injury. Neurobiol. Dis. 127, 570–581.
Hempstead, B.L., 2002. The many faces of p75NTR. Curr. Opin. Neurobiol. 12, 260–267.
Henriques, A., Pitzer, C., Schneider, A., 2010. Neurotrophic growth factors for the treatment of amyotrophic lateral sclerosis: where do we stand? Front. Neurosci. 4, 32.
Hu, Y., Cho, S., Goldberg, J.L., 2010. Neurotrophic effect of a novel TrkB agonist on retinal ganglion cells. Invest. Ophthalmol. Vis. Sci. 51, 1747–1754.
Huang, E.J., Reichardt, L.F., 2001. Neurotrophins: roles in neuronal development and function. Annu. Rev. Neurosci. 24, 677–736.
Huang, E.J., Reichardt, L.F., 2003. Trk receptors: roles in neuronal signal transduction. Annu. Rev. Biochem. 72, 609–642.
Ibanez, C.F., 1998. Emerging themes in structural biology of neurotrophic factors. Trends Neurosci. 21, 438–444.
Ibáñez, C.F., Simi, A., 2012. p75 neurotrophin receptor signaling in nervous system injury and degeneration: paradox and opportunity. Trends Neurosci. 35, 431–440.
Jang, S.-W., Liu, X., Yepes, M., Shepherd, K.R., Miller, G.W., Liu, Y., Wilson, W.D., Xiao, G., Blanchi, B., Sun, Y.E., et al., 2010. A selective TrkB agonist with potent neurotrophic activities by 7,8-dihydroxyflavone. Proc. Natl. Acad. Sci. 107, 2687.

Ji, Y., Lu, Y., Yang, F., Shen, W., Tang, T.T., Feng, L., Duan, S., Lu, B., 2010. Acute and gradual increases in BDNF concentration elicit distinct signaling and functions in neurons. Nat. Neurosci. 13, 302–309.
Kaplan, D.R., Miller, F.D., 2000. Neurotrophin signal transduction in the nervous system. Curr. Opin. Neurobiol. 10, 381–391.
Kim, G.S., Cho, S., Nelson, J.W., Zipfel, G.J., Han, B.H., 2014. TrkB agonist antibody pretreatment enhances neuronal survival and long-term sensory motor function following hypoxic ischemic injury in neonatal rats. PLoS ONE 9 (e88962-e88962).
Kishino, A., Ishige, Y., Tatsuno, T., Nakayama, C., Noguchi, H., 1997. BDNF prevents and reverses adult rat motor neuron degeneration and induces axonal outgrowth. Exp. Neurol. 144, 273–286.
Knusel, B., Gao, H., Okazaki, T., Yoshida, T., Mori, N., Hefti, F., Kaplan, D.R., 1997. Ligand-induced down-regulation of Trk messenger RNA, protein and tyrosine phosphorylation in rat cortical neurons. Neuroscience 78, 851–862.
Lagier-Tourenne, C., Polymenidou, M., Hutt, K.R., Vu, A.Q., Baughn, M., Huelga, S.C., Clutario, K.M., Ling, S.C., Liang, T.Y., Mazur, C., et al., 2012. Divergent roles of ALS-linked proteins FUS/TLS and TDP-43 intersect in processing long pre-mRNAs. Nat. Neurosci. 15, 1488–1497.
Leibrock, J., Lottspeich, F., Hohn, A., Hofer, M., Hengerer, B., Masiakowski, P., Thoenen, H., Barde, Y.A., 1989. Molecular cloning and expression of brain-derived neurotrophic factor. Nature 341, 149–152.
Lewin, G.R., Barde, Y.A., 1996. Physiology of the neurotrophins. Annu. Rev. Neurosci. 19, 289–317.
Lin, Z., Tann, J.Y., Goh, E.T., Kelly, C.E., Lim, K.B., Gao, J.F., Ibanez, C.F., 2015. Structural basis of death domain signaling in the p75 neurotrophin receptor. Elife 4 (11692–11692).
Longo, F.M., Massa, S.M., 2013. Small-molecule modulation of neurotrophin receptors: a strategy for the treatment of neurological disease. Nat. Rev. Drug Discov. 12, 507.
Lowry, K.S., Murray, S.S., Mclean, C., Talman, P., Mathers, S., Lopes, E.C., Cheema, S.S., 2001. A potential role for the p75 low-affinity neurotrophin receptor in spinal motor neuron degeneration in murine and human amyotrophic lateral sclerosis. Amyotroph. Lateral Scler. 2, 127–134.
Lu, B., Pang, P.T., Woo, N.H., 2005. The yin and yang of neurotrophin action. Nat. Rev. Neurosci. 6, 603–614.
Lu, B., Nagappan, G.H., Guan, X.M., Nathan, P.J., Wren, P., 2013. BDNF-based synaptic repair as a disease-modifying strategy for neurodegenerative diseases. Nat. Rev. Neurosci. 14, 401–416.
Matusica, D., Alfonsi, F., Turner, B.J., Butler, T.J., Shepheard, S.R., Rogers, M.-L., Skeldal, S., Underwood, C.K., Mangelsdorf, M., Coulson, E.J., 2016. Inhibition of motor neuron death in vitro and in vivo by a p75 neurotrophin receptor intracellular domain fragment. J. Cell Sci. 129, 517.
Merkouris, S., Barde, Y.-A., Binley, K.E., Allen, N.D., Stepanov, A.V., Wu, N.C., Grande, G., Lin, C.-W., Li, M., Nan, X., et al., 2018. Fully human agonist antibodies to TrkB using autocrine cell-based selection from a combinatorial antibody library. Proc. Natl. Acad. Sci. U. S. A. 115, E7023–E7032.
Mitchell, J.D., Borasio, G.D., 2007. Amyotrophic lateral sclerosis. Lancet 369, 2031–2041.
Morse, J., Wiegand, S., Anderson, K., You, Y., Cai, N., Carnahan, J., Miller, J., DiStefano, P., Altar, C., Lindsay, R., 1993. Brain-derived neurotrophic factor (BDNF) prevents the degeneration of medial septal cholinergic neurons following fimbria transection. J. Neurosci. 13, 4146–4156.
Mutoh, T., Sobue, G., Hamano, T., Kuriyama, M., Hirayama, M., Yamamoto, M., Mitsuma, T., 2000. Decreased phosphorylation levels of TrkB neurotrophin receptor in the spinal cords from patients with amyotrophic lateral sclerosis. Neurochem. Res. 25, 239–245.
Nagahara, A.H., Tuszynski, M.H., 2011. Potential therapeutic uses of BDNF in neurological and psychiatric disorders. Nat. Rev. Drug Discov. 10, 209–219.
Nagappan, G., Lu, B., 2005. Activity-dependent modulation of the BDNF receptor TrkB: mechanisms and implications. Trends Neurosci. 28, 464–471.
Neurology, 1999. A controlled trial of recombinant methionyl human BDNF in ALS. Neurology 52 (1427–1427).
Nykjaer, A., Willnow, T.E., Petersen, C.M., 2005. p75NTR—live or let die. Curr. Opin. Neurobiol. 15, 49–57.
Ochs, G., Penn, R.D., York, M., Giess, R., Beck, M., Tonn, J., Haigh, J., Malta, E., Traub, M., Sendtner, M., et al., 2000. A phase I/II trial of recombinant methionyl human brain derived neurotrophic factor administered by intrathecal infusion to patients with amyotrophic lateral sclerosis. Amyotroph. Lateral Scler. Other Motor Neuron Disord. 1, 201–206.
Poduslo, J.F., Curran, G.L., 1996. Permeability at the blood-brain and blood-nerve barriers of the neurotrophic factors: NGF, CNTF, NT-3, BDNF. Mol. Brain Res. 36, 280–286.
Qian, M.D., Zhang, J., Tan, X., Wood, A.R., Gill, D.S., Cho, S., 2006. Novel agonist monoclonal antibodies activate TrkB receptors and demonstrate potent neurotrophic activities. J. Neurosci. 26, 9394–9403.
Qiu, H.Y., Lee, S., Shang, Y.L., Wang, W.Y., Au, K.F., Kamiya, S., Barmada, S.J., Finkbeiner, S., Lui, H.S., Carlton, C.E., et al., 2014. ALS-associated mutation FUS-R521C causes DNA damage and RNA splicing defects. J. Clin. Investig. 124, 981–999.
Reichardt, L.F., 2006. Neuratrophin-regulated signalling pathways. Philos. Trans. R Soc. Lond. B Biol. Sci. 361, 1545–1564.
Roberson, M.D., Toews, A.D., Bouldin, T.W., Weaver, J., Goines, N.D., Morell, P., 1995. NGFR-mRNA expression in sciatic nerve: a sensitive indicator of early stages of axonopathy. Brain Res. Mol. Brain Res. 28, 231–238.
Roopenian, D.C., Akilesh, S., 2007. FcRn: the neonatal Fc receptor comes of age. Nat. Rev. Immunol. 7, 715.
Ruven, C., Chan, T.-K., Wu, W., 2014. Spinal root avulsion: an excellent model for studying motoneuron degeneration and regeneration after severe axonal injury. Neural Regen. Res. 9, 117–118.
Sakane, T., Pardridge, W.M., 1997. Carboxyl-directed pegylation of brain-derived neurotrophic factor markedly reduces systemic clearance with minimal loss of biologic activity. Pharm. Res. 14, 1085–1091.
Sasaki, S., Shibata, N., Iwata, M., 2001. Neuronal nitric oxide synthase immunoreactivity in the spinal cord in amyotrophic lateral sclerosis. Acta Neuropathol. 101, 351–357.
Sendtner, M., Holtmann, B., Kolbeck, R., Thoenen, H., Barde, Y., 1992. Brain-derived neurotrophic factor prevents the death of motoneurons in newborn rats after nerve section. Nature 360, 757–759.
Shepheard, S.R., Chataway, T., Schultz, D., Rush, R.A., Rogers, M., 2014. The extracellular domain of neurotrophin receptor p75 as a candidate biomarker for amyotrophic lateral sclerosis. PLoS ONE 9.
Shruthi, S., Sumitha, R., Varghese, A.M., Ashok, S., Chandrasekhar Sagar, B.K., Sathyaprabha, T.N., Nalini, A., Kramer, B.W., Raju, T.R., Vijayalakshmi, K., et al., 2017. Brain-derived neurotrophic factor facilitates functional recovery from ALS-cerebral spinal fluid-induced neurodegenerative changes in the NSC-34 motor neuron cell line. Neurodegener. Dis. 17, 44–58.
Soderquist, R.G., Milligan, E.D., Sloane, E.M., Harrison, J.A., Douvas, K.K., Potter, J.M., Hughes, T.S., Chavez, R.A., Johnson, K., Watkins, L.R., et al., 2009. PEGylation of brain-derived neurotrophic factor for preserved biological activity and enhanced spinal cord distribution. J. Biomed. Mater. Res. A 91, 719–729.
Todd, D., Gowers, I., Dowler, S.J., Wall, M.D., Mcallister, G., Fischer, D.F., Dijkstra, S., Fratantoni, S.A., De Bospoort, R.V., Veenmankoepke, J., 2014. A monoclonal antibody TrkB receptor agonist as a potential therapeutic for Huntington's disease. PLoS ONE 9.
Traub, S., Stahl, H., Rosenbrock, H., Simon, E., Florin, L., Hospach, L., Hörer, S., Heilker, R., 2017. Pharmaceutical characterization of tropomyosin receptor kinase B-agonistic antibodies on human induced pluripotent stem (hiPS) cell-derived neurons. J. Pharmacol. Exp. Ther. 361, 355–365.
Turner, B.J., Cheah, I.K., Macfarlane, K.J., Lopes, E.C., Petratos, S., Langford, S.J., Cheema, S.S., 2003. Antisense peptide nucleic acid-mediated knockdown of the p75 neurotrophin receptor delays motor neuron disease in mutant SOD1 transgenic mice. J. Neurochem. 87, 752–763.
Turner, B.J., Murray, S.S., Piccenna, L., Lopes, E.C., Kilpatrick, T.J., Cheema, S.S., 2004. Effect of p75 neurotrophin receptor antagonist on disease progression in transgenic amyotrophic lateral sclerosis mice. J. Neurosci. Res. 78, 193–199.
Tuszynski, M.H., Mafong, E., Meyer, S., 1996. Central infusions of brain-derived neurotrophic factor and neurotrophin-4/5, but not nerve growth factor and neurotrophin-3, prevent loss of the cholinergic phenotype in injured adult motor neurons. Neuroscience 71, 761–771.
Ultsch, M.H., Wiesmann, C., Simmons, L.C., Henrich, J., Yang, M., Reilly, D., Bass, S.H., De Vos, A.M., 1999. Crystal structures of the neurotrophin-binding domain of TrkA, TrkB and TrkC. J. Mol. Biol. 290, 149–159.
Vilar, M., Charalampopoulos, I., Kenchappa, R.S., Simi, A., Karaca, E., Reversi, A., Choi, S., Bothwell, M., Mingarro, I., Friedman, W.J., 2009. Activation of the p75 neurotrophin receptor through conformational rearrangement of disulphide-linked receptor dimers. Neuron 62, 72–83.
Wiese, S., Herrmann, T., Drepper, C., Jablonka, S., Funk, N., Klausmeyer, A., Rogers, M.L., Rush, R., Sendtner, M., 2010. Isolation and enrichment of embryonic mouse motoneurons from the lumbar spinal cord of individual mouse embryos. Nat. Protoc. 5, 31–38.
Woo, N.H., Teng, H.K., Siao, C.J., Chiaruttini, C., Pang, P.T., Milner, T.A., Hempstead, B.L., Lu, B., 2005. Activation of p75NTR by proBDNF facilitates hippocampal long-term depression. Nat. Neurosci. 8, 1069–1077.
Wu, W., 1996. Potential roles of gene expression change in adult rat spinal motoneurons following axonal injury: a comparison among c-Jun, low-affinity nerve growth factor receptor (LNGFR), and nitric oxide synthase (NOS). Exp. Neurol. 141, 190–200.
Wu, W., Liuzzi, F.J., Schinco, F.P., Depto, A.S., Li, Y., Mong, J.A., Dawson, T.M., Snyder, S.H., 1994. Neuronal nitric oxide synthase is induced in spinal neurons by traumatic injury. Neuroscience 61, 719–726.
Wu, W., Li, L., Yick, L., Chai, H., Xie, Y., Yang, Y., Prevette, D., Oppenheim, R.W., 2003. GDNF and BDNF Alter the Expression of Neuronal NOS, c-Jun, and p75 and Prevent Motoneuron Death following Spinal Root Avulsion in Adult Rats. J. Neurotrauma 20, 603–612.
Yan, Q., Elliott, J.L., Snider, W.D., 1992. Brain-derived neurotrophic factor rescues spinal motor neurons from axotomy-induced cell death. Nature 360, 753–755.
Yanpallewar, S.U., Barrick, C.A., Buckley, H., Becker, J., Tessarollo, L., 2012. Deletion of the BDNF truncated receptor TrkB.T1 delays disease onset in a mouse model of amyotrophic lateral sclerosis. PLoS ONE 7 (e39946-e39946).